HYDROGEN INDUCED SURFACE CRACKING OF TWO ORTHOPEDIC IMPLANT ALLOYS

by

Ray C. Wasielewski

Thesis submitted to the faculty of Virginia Tech
in partial fulfillment of the requirements for the degree of

MASTERS OF SCIENCE
in
Materials Engineering

APPROVED:

M. R. Louthan, Jr., Chairman

W. R. Hibbard

J. L. Lytton

June, 1982

Blacksburg, Virginia

ACKNOWLEDGEMENTS

The author wishes to extend his most sincere thanks to his committee chairman, Dr. M. R. Louthan Jr., for his guidence and support which were instrumental throughout this undertaking. Also, thanks are due for my committee members, Dr. W. R. Hibbard Jr., Dr. J. L. Lytton, and Dr. D. W. Dwight, for their conscientious but critical review of the materials in this thesis.

Special thanks are also in order for: T. S. Sudarshan for his help proof reading this text for errors, Brian Edwards for allowing me to use several negatives from his thesis report, Mark Buchnam for his instruction on using CMS Script, and Deforrest Hipps for his advice on the photographic work contained in this project. Also, many thanks are due to my fellow graduate students, John Wagner, Bill Spacciapoli, Scott Milkovich, Joe Terrell, and Eric Hoffman, for many helpful discussions of the materials and data presented in this report. Also, to Cindy Kornegay and Rick Louthan for their help in preparing the many samples utilized for testing. The financial support of the Department of Energy under contract DE-AS-05-78-ER-06039 is also gratefully acknowledged.

The author would like to sincerely express his deep gratitude and thanks to the secretaries of the Materials

Engineering Department: Jeanne Warner, Karen Kessinger, and Jamie Stokes, for their countless services rendered throughout this endeavor.

And finally, the author wishes to thank his family: my father and mother Gerald and Margaret Wasielewski; and my brothers and sisters Janice, Marianne, Michele, Craig and Karen. Their constant love, understanding, and support are an inspiration to me, and have been vital to the fulfillment and enjoyment of my educational studies.

TABLE OF CONTENTS

LIST OF FIGURES

LIST OF FIGURES (cont.)

LIST OF FIGURES (cont.)

LIST OF TABLES

I. INTRODUCTION

The medical profession utilizes a wide variety of materials to repair and replace portions of the musculoskeletal system. Since the late 1920's, stainless steel has been used extensively in internal fixation and replacement prostheses, and today is the most predominant implant alloy.[1] Cobalt- chromium- molybdenum alloys have been used since the late 1930's, and today are the most common material for hip replacement prosthesis.[2] The cobalt based alloy and stainless steel utilized frequently in current implant devices are H.I.P. ZIMALOY (registered trade name of Zimmer USA) and 316 stainless steel, respectively. Surgical implants made of these materials have shown good biocompatibility when implanted in the body. Increases in service life however, have placed an increasing demand on in vivo material performance,[3] and caused increasing concerns over the long term reliability of these alloys in the body fluids.

When materials are surgically placed in the body, failure can be induced by several possible modes. Corrosion and fatigue, acting seperately or in conjunction, have been most frequently cited as responsible for in vivo implant failure.[1 4 5] Recently it has been demonstrated however, that conditions present in the body are conducive to

electrolytic hydrogen formation,[6] and to subsequent cathodic charging of implanted materials.[7] The long time occurrence of this phenomenon would greatly degrade the in vivo performance of 316 stainless steel,[8-15] and H.I.P. ZIMALOY implants.[7] Such degradation is expected because of the documented susceptibility of these alloys to mechanical property losses during hydrogen exposure.

Studies were therefore conducted to investigate the microstructural variables affecting hydrogen induced surface cracking of 316 stainless steel and H.I.P. ZIMALOY. The ability to relate the severity of surface cracking to certain microstructural features, will not only contribute to the development of improved surgical implant materials, but will significantly benefit the more general application of these materials in hydrogeneous environments.

II. LITERATURE REVIEW

Surgical implants are the tools of the orthopedic surgeon used most frequently to mend fractures or replace worn or injured portions of the musculoskeletal system. The mechanical and chemical environment associated with in vivo applications adds complexity to the design and selection requirements of implanted materials. Recent innovations in surgical techniques allow metal implants to be adapted for nearly permanent functions as substitutional limbs and joints. This increase in life expectancy however has caused a corresponding increase in the occurrence of implant failure, and subsequently an increase in the need to improve the compatibility of in vivo implant materials with body fluids.

A. Implant Material Requirements

Irrespective of the method of internal fixation or replacement, or of the devices used, certain physical properties of implant devices must be considered. The chemical composition of the material for the implant is of utmost importance. Mechanical strength and inertness in body fluids must be demonstrated for any material used in surgical implantation. The chemical composition and

mechanical properties of 316 stainless and H.I.P. ZIMALOY studied in this investigation, are listed in Tables 1 and 2, and will be subsequently discussed.

The requirement that surgical implants be inherently corrosion resistant and chemically inert in vivo, is a difficult metallurgical task. Consideration of the aggressive nature of the body into which implants are inserted, gives a better understanding of the necessity for stringent material requirements.

Body fluids are aqueous, salty chloride containing solutions, and therefore augment electron transfer and promote electrochemical processes, such as corrosion. The solution pH is also significant in electrolytic processes, and ranges from a pH of 5 (post surgery or due to infection) to a pH of about 9 (hematoma).[16] This variance can greatly alter the corrosive nature of the environment to which implants are exposed.[1 17 18] Design of surgically implanted devices must therefore consider material compatibility with these body fluids.

316 stainless steel is most commonly used as fixation devices for bone fracture repair, but continues to find permanent use in skeletal support pins and joint protheses. The major reason that 316 stainless steel is chosen for body implantation, is the ability of this alloy to withstand

TABLE #1

CHEMICAL ANALYSIS OF 316 STAINLESS STEEL

AND

H.I.P. ZIMALOY

	AISI Type 316+	H.I.P. ZIMALOY++
C	0.08(max)	0.024
P	0.045(max)	0.011
S	0.030(max)	0.012
Mn	2.00(max)	0.41
Si	1.00(max)	0.75
Cr	16.0-18.0	29.1
Ni	10.0-14.0	0.18
Mo	2.00-3.00	6.28
Fe	Balance	0.10
W	-------	0.054
Cu	-------	0.015
Co	-------	Balance

+ Values Acquired from reference #[19]

++ Values Acquired from reference #[20]

TABLE #2

MECHANICAL PROPERTIES OF TYPICAL

316 STAINLESS STEEL AND H.I.P.ZIMALOY

ORTHOPEDIC IMPLANT ALLOYS

	Ultimate Tensile Strength (Mpa/Ksi)	Yield Strength (Mpa/Ksi)	% Elongation	% Reduction of Area
316 Stainless Steel (annealed)[+]	579/84	262/38	68	78
316 Stainless Steel (HERFed)[++]	862/125	689/100	14	65
H.I.P. ZIMALOY[+++]	1295/188	916/133	14	16
Cast ZIMALOY[+++]	723/105	517/75	8	8

[+]Values Acquired From Reference #[10]

[++]Values Acquired From Reference #[13]

[+++]Values Acquired From Reference #[20]

pitting and crevice corrosion in vivo, in the chloride containing body fluids.[1 21 22]

The corrosion resistant properties of stainless steels are mainly imparted by chromium (>16%), which under normal conditions forms a self healing continuous layer of oxide over the surface of the material. This oxide serves to insulate the material from its environment.[23] The addition of nickel (>11%) also aids in corrosion resistance. Nickel increases the stability of austenite (γ), and suppresses the formation of alpha ferrite (α). Nickel content (>8%) also inhibits martensitic transformations. The presence of martensite or a second phase (α), in the austenite matrix, would decrease corrosion resistance.[1] Molybdenum is added (>2%) to the 316 stainless steel to enhance the mechanical properties which were sacrificed by increasing the nickel content greater than 8%. Molybdenum however, has the undesirable effect of being a delta ferrite (δ) stabilizer. Therefore, a solutionizing anneal is required to dissolve this unwanted second phase (δ-ferrite) and maximize corrosion resistance. Maintaining nickel (γ promoter) on the high side of specification limits, and maintaining chromium (a ferrite stabilizer) proximal to its specification minimum, also helps eliminate the possibility of delta ferrite formation, and supplements corrosion resistance.[1 23]

H.I.P. ZIMALOY has superior corrosion resistance, fatigue strength, and abrasion resistance, relative to 316 stainless steel, and is therefore a frequently recommended material for permanent implant devices.[2 4 16 24] The alloying element that controls the corrosion resistance of H.I.P. ZIMALOY is chromium. The importance of chromium in this corrosion resistant application, is the formation of a passive film consisting mainly of hydrated chromium oxy-hydroxide.[25] The integrity of these chromium rich films inhibits the corrosion of the underlying material, forming a protective film around the implant. The protective character of this film increases as the chrome content is increased. The mechanical integrity of Co- Cr- Mo alloys are significantly influenced by the presence of carbides. The presence of various chromium, chromium- molybdenum, and other carbides - usually of the M_7C_3 and $M_{23}C_7$ type - results in a considerable degree of strengthening, and a reasonable amount of ductility if the carbides are interdendritically dispersed as discrete particles.[4]

The mechanical integrity of implanted devices is an important materials consideration, because such devices are frequently exposed to load bearing conditions as structural components, or as support devices for portions of the musculoskeletal system. While the extent and nature of

implant load exposure is dependent on the application, the various forms of normal muscle and skeletal motion (even subtle changes in posture) can subject any implanted device to a wide range and frequency of loads.[5] For instance, walking can load an implanted hip prosthesis to several times the body weight,[26] and the loads on other devices are frequently of similar magnitude. Thus, normal body movement in conjunction with the facts that implanted materials are of limited dimension, and that loading and unloading can occur millions of times, causes significant mechanical demands with respect to fatigue.

The problems of fatigue however, are further complicated by the detrimental nature of the in vivo environment into which prothesis devices are surgically placed. Therefore, the combined effects of mechanical loading, of chemical interaction, and of extended implant life, have resulted in an increase in the frequency of implant failure, which are often attributed to corrosion fatigue.[27] [28] Hydrogen environments are well known to accelerate fatigue processes, and have been related to failure of implanted devices.[7] This is especially true of hydrogen generated cathodically in vivo during typical corrosion processes,[6] which could cause the surface of an implanted alloy to develop shallow surface cracks.[8] [14] These

surface cracks could then substantially degrade the fatigue resistence of an implanted material by providing the stress intensity necessary for fatigue crack initiation. Thus an increased understanding of hydrogen compatibility, may lead to an increased understanding of the failure process for implant materials, as discussed in the next section.

B. Hydrogen Induced Surface Cracking

Cobalt- chromium- molybdenum alloys and austenitic stainless steels, are used extensively in the medical profession as orthopedic implant materials. The suitability of both alloys to use in the body, lies in their inherent corrosion resistance, and in their ability to retain mechanical integrity long after implantation. The increase in implant life expectancy however, has caused a corresponding increase in the occurrence of implant failures.

Implant failures have been attributed to fatigue,[17 28-33] corrosion,[1 4 6 22 28 34-38] corrosion fatigue,[21 24 27 28 39 40] and to stress corrosion cracking.[21 24 40] Several investigators have attempted to evaluate the fracture mechanism, through the analysis of fracture surfaces in these implants.[40 41] The difficultly in distiguishing

between the different failure modes, and the frequent contributions of several fracture processes, have lead to the contention that several different mechanisms act simultaneously - in conjunction - to cause implant failures.[39 42 43]

One possible mechanism involves the contribution of hydrogen embrittlement to implant failures. A recent study has shown that hydrogen induces ductility losses in H.I.P. ZIMALOY, and that hydrogen embrittlement could contribute to common implant failure modes.[7] It was found that after 2 months in a Ringers solution (a synthetic body fluid used to simulate in vivo conditions), the corrosion potential of ZIMALOY in a creviced condition shifted 150mV active, with respect to ZIMALOY in the non-creviced condition.[7] This supported a similar observation by Levine and Staehl, with creviced 316 stainless steel.[6] Such shifts in potential would cause an implanted material to become cathodic, and subsequently have hydrogen discharged at the surface, similar to cathodic hydrogen evolution in an electrochemical cell. This effect can be simulated, by making the test material the cathode in an electrochemical cell utilizing

the desired electrolyte. Hydrogen is subsequently generated at the sample surface by the reaction,

$$H^+ + e^- \text{ ------> } H(ads)$$

and some of the generated hydrogen can be absorbed by the sample.

$$H(ads) \text{ ------> } H(abs)$$

Studies on the effects of cathodic charging on the behavior of stainless steels are extensive in the literature.[8 9 14 15 44-51] Investigations have shown that electrolytic charging of hydrogen into samples in the absence of externally applied stress, frequently induces surface cracking.[8 14 15 44-49] Data suggests that during charging, hydrogen is forced into samples at very high external fugacity. Extreme supersaturation of the surface layer results when charging is stopped. This supersaturation concentrates hydrogen at the microvoids and other volume defects, and forms gaseous internal hydrogen bubbles. The internal gaseous hydrogen pressure, results in formation of severe strains retained in the metal lattice.

Previous investigators have qualitatively measured these strains through the use of X-ray diffractive analysis.[44] The diffraction peaks for uncharged samples were

found to be sharp, but the peaks broadened and shifted to lower angles (lattice expansion) after hydrogen charging. This broadening and shifting of peaks is associated with the high internal hydrogen content that develops during cathodic charging, and results from the positive partial molar volume of hydrogen in solution.

Surface cracking of cathodically charged samples is a phenomena that frequently occurs after charging ceases. This time dependent change is termed an aging process, and is a means of dissipating the lattice strain energy associated with the expansion, and the attempts of the lattice to contract as hydrogen outgassing takes place. As the sample ages at room temperature, cracking initiates, continuing until the strain energy is no longer sufficient to form new crack surfaces, and equilibrium conditions are obtained. Several investigators have noted,[8 14 45-47] or studied,[15 44 48] the effects of outgassing time, on the severity of surface cracking that results after cathodic charging. These studies consider the importance of aging effects, and demonstrate how subsequent errors can be avoided by conducting surface measurements after equilibrium conditions have been reached.

In this investigation the time dependent severity of surface cracking was determined to justify conclusions

reached in this report. The effects of outgassing time was therefore addressed, and all photomicrographs used in this report (except where noted otherwise) were taken after surface cracking had reached equilibrium conditions at room temperature. The actual time dependence of cracking, as well as further discussion of aging effects, are presented in section IV (A) of this report.

C. Microstructure and Hydrogen Compatibility

The increase in life expectancy of surgical implants has placed more stringent requirements on mechanical integrity and corrosion resistance of implanted materials. Variations in the processing of existing alloys have been utilized to increase the compatibility of materials with body fluids. For the most part, changes in processing have been utilized to improve mechanical properties, and since composition is not changed, the alloy generally retains its clinically proven chemical compatibility. The effects of annealing,[16 21] sensitizing,[21 37] HERFing,[24] thermomechanical processing,[16] and Hot Isostatic Pressing[2 23] on in vitro material performance have been investigated. The improvement in mechanical properties, and subsequent fatigue resistance, is most promising in the areas of

H.I.P., HERFing, and other thermomechanical processing techniques.

These processing changes however, have also been shown to affect the severity of degradation that results during hydrogen exposure.[7 13 52-54] While work has been done to investigate the change in the hydrogen compatibility of an alloy due to variations in processing, the basic microstructure justification for these changes has not been established. It is therefore the purpose of this study to determine the hydrogen compatibility of various 316 stainless steel and ZIMALOY microstructural features (susceptibility to surface cracking). By establishing those microstructural feature responsible for augmenting the extent of surface cracking during cathodic hydrogen exposure, changes in processing can be utilized to avoid these structures, and at the same time improve mechanical integrity. Therefore, materials with proven biocompatibility could be processed in a manner to achieve both maximum hydrogen and mechanical compatibility. This would result in an increase in the reliability of these materials for utilization in the body. Also, This ability to control hydrogen compatibility through processing changes will not only be important in controlling the contribution of hydrogen damage in implant failure, but will be very

significant in controlling the compatibility of any material exposed to a hydrogen environment.

Most implant failures in the literature have cited fatigue or fatigue aided degradation of implanted devices, as the major reason for failure. In orthopedic hip prostheses, fatigue failure is found to initiate at the anterolateral portion of the stem.[17] The crack then procedes medially in a low cycle fatigue mode, and then by rapid failure once the surface area has been reduced sufficiently (by some critical amount of crack growth), such that the applied load is greater than the strength of the material.[55]

Fracture induced stem breakage as well as other failures related to mechanical property inadequacies, has stimulated the study and use of processing techniques to obtain improved fatigue properties. Hot Isostatic Pressing of Co- based alloys and HERFing 316 stainless steel, are two possible methods of increasing the fatigue and yield strength of implanted devices. These changes in processing, without compositional variation, result in devices whose inherent corrosion resistance is unchanged, but whose mechanical properties are improved.

Lack of metal fatigue strength, and the presence of metallurgical defects, have been implicated in some failures of investment cast femoral prostheses.[31] An approach to

improving the strength characteristics of Co- Cr- Mo is to fabricate implant devices by processing very clean atomized alloy powders. The solidification rates developed during powder atomization are several orders of magnitude greater than that developed during investment casting.[2] This allows the large grain size of investment cast prostheses to be replaced by a very fine grained H.I.P. microstructure. Metallographic examination of H.I.P. ZIMALOY used in this investigation, revealed an ultra fine grain size and a very uniform dispersion of small carbide particles. The H.I.P. ZIMALOY has vastly improved strength properties (see Table 2), and a fatigue strength of more than twice that of cast ZIMALOY.[20] The increased fatigue resistance implies that prostheses, fabricated by the H.I.P. process, could withstand higher loads and a larger number of cycles before fatigue becomes a problem. This processing technique also permits the utilization of the same alloy composition, that has been demonstrated to be clinically biocompatible for decades. Therefore, mechanical compatibility of Co- based implants can benefit from the H.I.P. process without any loss in chemical compatibility.

The effect of H.I.P. on hydrogen compatibility would also appear to be favorable. Edwards found that cast ZIMALOY samples were more susceptible to hydrogen induced

property losses, than were H.I.P. ZIMALOY samples.[7] As previously stated, the consolidation of alloy powders at a temperature below the melting point of the alloy, results in a very fine grain size as compared to conventional cast prostheses. A decrease in grain size has been shown to generally increase the hydrogen compatibility of metals.[5,6] Therefore, not only is H.I.P. significant for its improved fatigue properties, but this process produces a microstructure which is less susceptible to the detrimental effects of electrolytically induced surface cracking, caused by in vivo hydrogen generation.

High energy rate forming (HERFing), significantly increases the strength of austenitic stainless steels, and thereby expands the useful design range, and thus the applicability, of these typically strength limited alloys. For austenitic stainless steels, proper forging conditions can double the strength levels, while retaining good ductility (see Table 2). This allows for either large increases in the allowable design stresses, or a reduction in section thickness. Therefore, the property modifications brought about by HERFing could contribute to improved implant design and integrity, as well as having a similar wide spead commercial significance.

For orthopedic implant devices, HERFing has been suggested as a means of increasing the fatigue resistance of implants, and allowing for a substantial reduction in size. In addition to this effect however, HERFing could improve the hydrogen compatibility of 316 stainless steel implant devices.

Herf processes have been shown to decrease hydrogen induced property losses in 316 stainless steel,[13] as well as in several other 300 series austenitic steels.[10-13 52-54 57 58] In the environment in vivo, which can cause electrolytic hydrogen generation, these HERFed alloys could prove to be less susceptible to hydrogen induced property changes. Also, the fact that chemically different 300 series stainless steels are affected similarly by HERFing, suggest that there is a microstructural justification for hydrogen compatibility changes similar to that for the observed property changes. Because of the great variety of materials used in hydrogeneous environments (not only implant devices), the development of a microstructural justification for relative hydrogen compatibility will have widespread significance.

The prevention or minimization of hydrogen induced damage through processing changes which produce optimally hydrogen compatible microstructures, would greatly benefit

the surface sensitive fatigue performance of orthopedic implants. For instance, minimizing the extent of hydrogen induced surface cracking of in vivo implant devices could reduce the occurrence fatigue failures, because of the surface sensitive nature of fatigue processes. The possible significance of preventing surface cracking in industrial applications is also similarly apparent, and would be of vital importance in commercial applications where fatigue resistance and hydrogen compatibility are required.

The effects of microstructure on the relative hydrogen compatibility of sensitized and annealed stainless steels are well documented. The general trend throughout the literature is as follows: sensitized materials are found to be least compatible in hydrogen environments; followed by annealed materials; and HERFed materials are the least susceptible. Sensitization processes have also been know to increase the susceptibility of austenitic steels to intergranular attack. This, in conjuction with the detrimental effects of surface cracking that could occur in vivo, suggests that sensitized material is not biocompatible relative to stainless steel processed to other conditions. Annealed materials, on the other hand, lie somewhere between the advantageous mechanical and chemical compatibility of HERFed materials, and the expected poor compatibility of

sensitized materials. As with HERFed materials, a correlation exists between hydrogen compatibility and whether a material is in the sensitized or annealed condition, regardless of alloy type or composition. This observation gives support to the contention that hydrogen compatibility is microstructurally controlled.

It would seem likely that changes in microstructure, brought about by changes in processing, could be a means of controlling the hydrogen compatibility of implanted 316 stainless steel and of ZIMALOY prostheses. It is therefore the purpose of this investigation to document the hydrogen compatibility of the different microstructures produced by different processing techniques. Once this has been accomplished, a microstructural justification for hydrogen compatibility can be established, and a microstructural methodology for controlling hydrogen effects in ZIMALOY and 316 stainless steel implants will logically follow.

III. METHODS AND MATERIALS

A. Materials and Sample Preparation

The 316 stainless steel used in this study was donated to the Materials Engineering Department at Virginia Tech by the Sandia Corporation, and was supplied in the HERF condition. The forged bar, 1/2" x 1/10" x 6" in dimensions had the composition given in Table 2, which also gives the composition of a Co based alloy, described in subsequent paragraphs. The forged bar was produced by a proprietary process of Precision Forge Corporation. Test samples were sectioned from the forged bar, and subsequently heat treated to produce the variant microstructures desired: annealed HERF in the recrystallized condition (A.HERF), sensitized HERF (S.HERF), annealed HERF which was sensitized (S.A.HERF), and the as received HERF (HERF). The heat treatments used to obtain each of these microstructures studied are given in Table 3.

The heat treated samples were mounted in liquid plastic, manually polished through 1 micron Al_2O_3 (alumina), and vibration finished using 0.05 micron alumina. In this manner a cognate surface finish was obtained on all samples. Samples were then cleaned using an acetone solvent, and

TABLE #3

316 STAINLESS STEEL

HEAT TREATMENTS

I. As Received HERF (HERF)

A. No Heat Treatment

II. Annealed HERF (A.HERF)

A. 1050°C for 1 hour

B. Air Cooled to Room Temperature

III. Sensitized HERF (S.HERF)

A. 650°C for 24 hours

B. Air Cooled to Room Temperature

IV. Sensitized Annealed HERF (S.A.HERF)

A. 1050°C for 1 hour

B. Then, 650°C for 24 hours

C. Air Cooled to Room Temperature

electrolytically etched under the following conditions:

Electrolyte ..... 10 grams Oxalic Acid

100 ml Distilled H_2O

Current Density ... $0.1A/cm^2$

Time ..... 1 minute The typical microstructures for HERF, S. HERF, A. HERF, and S.A. HERF 316 stainless steel samples are shown in Figures 1 - 4, respectively.

The Co- Cr- Mo surgical implant alloy used in this study - trade name ZIMALOY - was obtained from Zimmer U.S.A. in the form of scrap hip joint protheses, as shown in Figure 5+. The compositional analysis of H.I.P. ZIMALOY is given in Table 2. The stem portion of the implant (see arrow in Figure 5), was sectioned into 1/8" thick samples. ZIMALOY sample surfaces were prepared in exactly the same manner as 316 Stainless Steel samples.

Several different etching processes were utilized to characterize the ZIMALOY microstructure. A Vacuum Cathodic etching technique revealed the structure shown in Figure 6++, while an aqueous electrolytic etch with Sulfuric Acid, revealed the microstructures shown in Figure 7+.

+pictures courtesy of Brian Edwards (thesis report, 1981, V.P.I.)

++pictures courtesy of R. J. Grey, Oak Ridge National Laboratories, Oak Ridge, Tn.

Figure 1. Photomicrograph of HERF
316 stainless steel (200X)

High dislocation dense slip bands

High dislocation dense boundaries

Deformed twin boundaries

Figure 2. Photomicrograph of S.HERF 316 stainless steel (200X)

High dislocation dense slip bands

High dislocation dense boundaries

Deformed twin boundaries

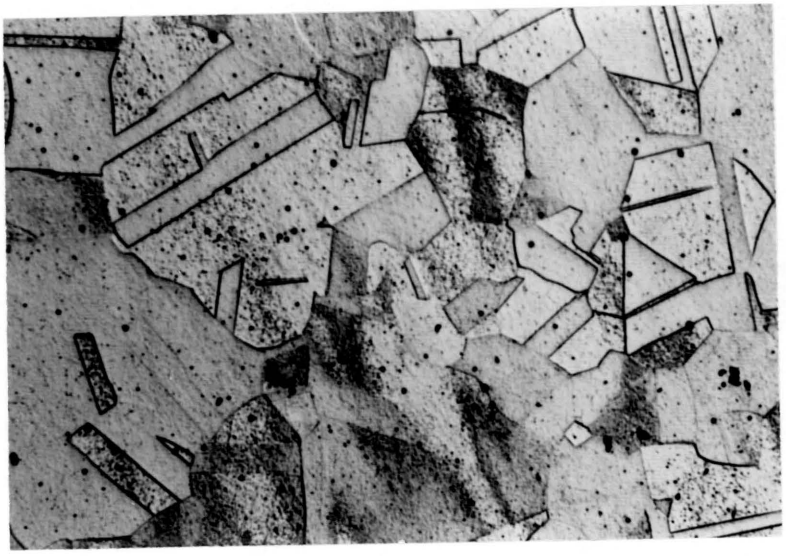

Figure 3. Photomicrograph of A.HERF 316 stainless steel (200X)

Twin boundaries

Grain boundaries

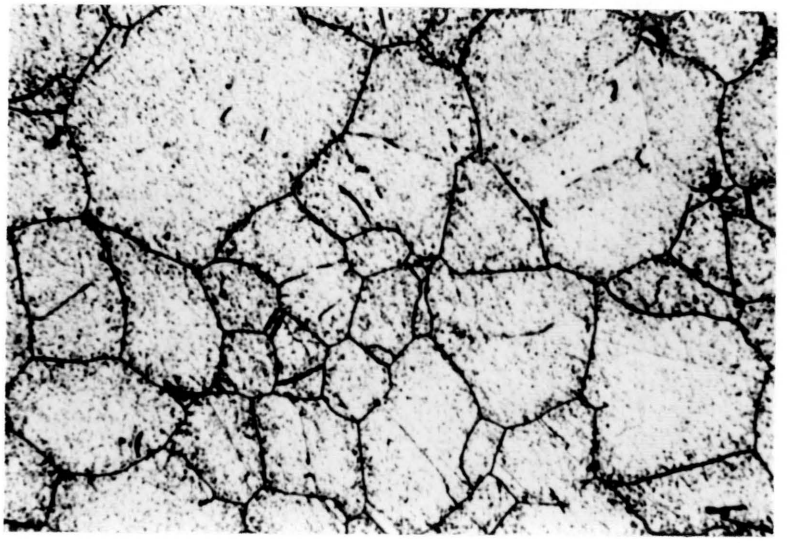

Figure 4. Photomicrograph of S.A.HERF 316 stainless steel (200X)

Twin boundaries

Grain boundaries

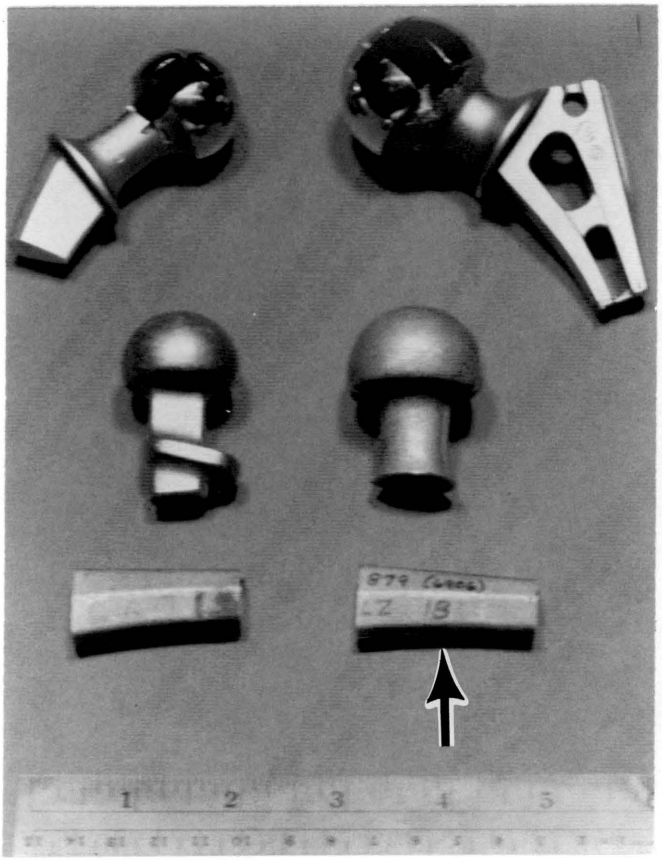

Figure 5. Photograph of scrap hip ZIMALOY prostheses orthopedic implant material as received from Zimmer

Stem portion

Figure 6. Differential interference contrast photomicrograph of vacuum cathodically etched ZIMALOY microstructure (5mA at 3.5 kV for 6 minutes)

Grain boundaries

Twin boundaries

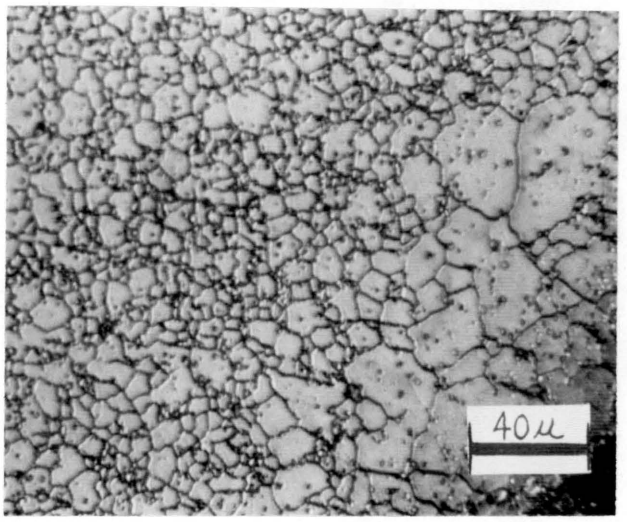

Figure 7. Photomicrograph of electrolytically etched H.I.P. ZIMALOY microstructure

Grain boundaries

Duplex grain structure

Carbide precipitates

B. Processing and Microstructure

The HERF 316 Stainless Steel used in this study was manufactured utilizing a proprietary process of Precision Forge. However, several significant generalizations can be made about HERFing processes, to facilitate an understanding of the microstructures investigated.

The 316 Stainless Steel pancake was ostensively produced by a closed die forging at temperatures in the vicinity of 980°C, and at deformation rates greater than the speed of sound. The elevated forging temperature effectively increases the toughness of the austenitic 316 stainless steel, so that it has sufficient ductility to accommodate the substantial amounts of strain energy induced in the sample during the HERFing process.

The significance of the high rate at which forging occurs can be demonstrated through the use of generalized dislocation mechanics and Equation 1.[59 60]

$$\gamma' = (\vec{b}) \times (\rho) \times \langle v \rangle \qquad (1)$$

Equation (1) relates the shear deformation rate (γ'), to the mobile dislocation density (ρ), the Burgers vector of the dislocation ($\vec{b}$), and on the average dislocation velocity $\langle v \rangle$. The process of HERFing produces shear strains, which must be compensated for through increases in the average velocity of dislocations, or an increase in the number of mobile dislocations. The energy required to increase the average velocity of dislocations moving at speeds less than the speed of sound, is frequently less than that required to activate new slip systems. Thus, normal processing generally increases the velocity of the dislocations. During HERFing however, the velocity of mobile dislocations approaches the speed of sound; the maximum possible dislocation velocity. And when the shear strain rate (γ') is too large to be accomodated solely through an increase in the average dislocation velocity $\langle v \rangle$, new slip systems are activated, and the mobile dislocation density (ρ) increases. The very high dislocation density induced by HERFing results in dense slip bands and deformed twins throughout the microstructure, and substantially increases the strength of the steel. The microstructural features, characteristic of HERFed materials, are shown in Figure 1. This micrograph however, shows that that there is a similarity between twins that have been deformed by the HERFing process and slip

bands in this microstructure. Therefore, to avoid any discrepancies in identification which may result, both these structures will be referred to as slip bands in this investigation.

The high dislocation density in HERFed materials also results in very high residual strain energy in the form of lattice defects. This defect structure - which is thermodynamically unstable - stores energy in the material, and provides the driving force for recovery and recrystallization. The thermal energy at room temperature however, is insufficient to initiate recovery and recrystallization processes, necessary for thermodynamic equilibrium to be obtained.[61]

Equilibrium conditions would require the release of energy by the local rearrangement of dislocation tangles, and the formation of low angle grain boundaries (>5°,<10°) and strain free grains.[59] [60] These processes, however, require dislocation climb, a diffusion controlled process, and are therefore thermally activated.

Annealing at a temperature of 1050°C provides the thermal energy input necessary for favorable diffusion kinetics, and subsequent recovery and recrystallization. This causes the dislocation dense slip bands to be removed from the sample, and new strain free grains to form. The

annealing temperature used in this study (1050°C) cause the dislocation dense slip bands and grain boundaries of a HERFed material (Figure 1), to transform into a structure which contained low energy grain boundaries and annealing twins (Figure 3), characteristic of annealed austenitic steels.

The available thermal energy at temperatures in the range of 650°C, is not sufficient to cause the degree of vacancy motion required for recrystallization, but are sufficient to cause precipitation of chrome carbidies at the boundary structures, in HERFed and A. HERFed materials. Sensitization - which is carbide precipitation - results from the 650°C anneal, and is clearly visible in the S.HERF and S.A. HERF microstructures of Figures 2 and 4, respectively.

The Cobalt based ZIMALOY used in this study was Hot Isostatically Pressed (H.I.P.) by the Zimmer Corporation. This process involves pressing an atomized mixture of Co-Cr-Mo powders at 1090°C and 103 MPa for 1 hour, thus allowing the particles to sinter by solid state diffusion. The resulting microstructure is shown in Figures 6 and 7.

The fine grain structure around the outer edges, is replaced by increasingly larger grain size, as the sample is traversed towards the center (see Figure 7). This

microstructure also contains a non-uniform distribution of carbide particles along the grain boundaries and within some grains. The presence of dispersed carbide particles along twins as well as grain boundaries is seen in Figure 6.

C. Hydrogen Charging and Surface Cracking

Hydrogen was introduced electrolytically (by Cathodic Charging) at current densities ranging from 0.01Amps/cm^2 to 0.5amp/cm^2, for times ranging between 1 and 24 hours, in the apparatus shown in Figure 8. The cell utilized a platinum anode, and an aqueous 1N Sulfuric Acid (H_2SO_4) electrolyte poisoned with 0.25 grams of Sodium Arsenite ($NaAsO_2$). Each sample was charged in 0.5 liters of fresh solution, and the electrolyte was gently agitated during charging using a magnetic stirring bar.

Cathodic charging induced surface cracking in all samples tested. Typical surface cracks that result after an A.HERF samples has been cathodically charged at 0.5A/cm^2 for 2 hours are shown in the scanning electron micrographs (S.E.M.) in Figure 9. Other photomicrographs presented in this report also illustrate similar cracking, however, the excellent depth of focus inherent of the scanning electron microscope produces micrographs which more clearly

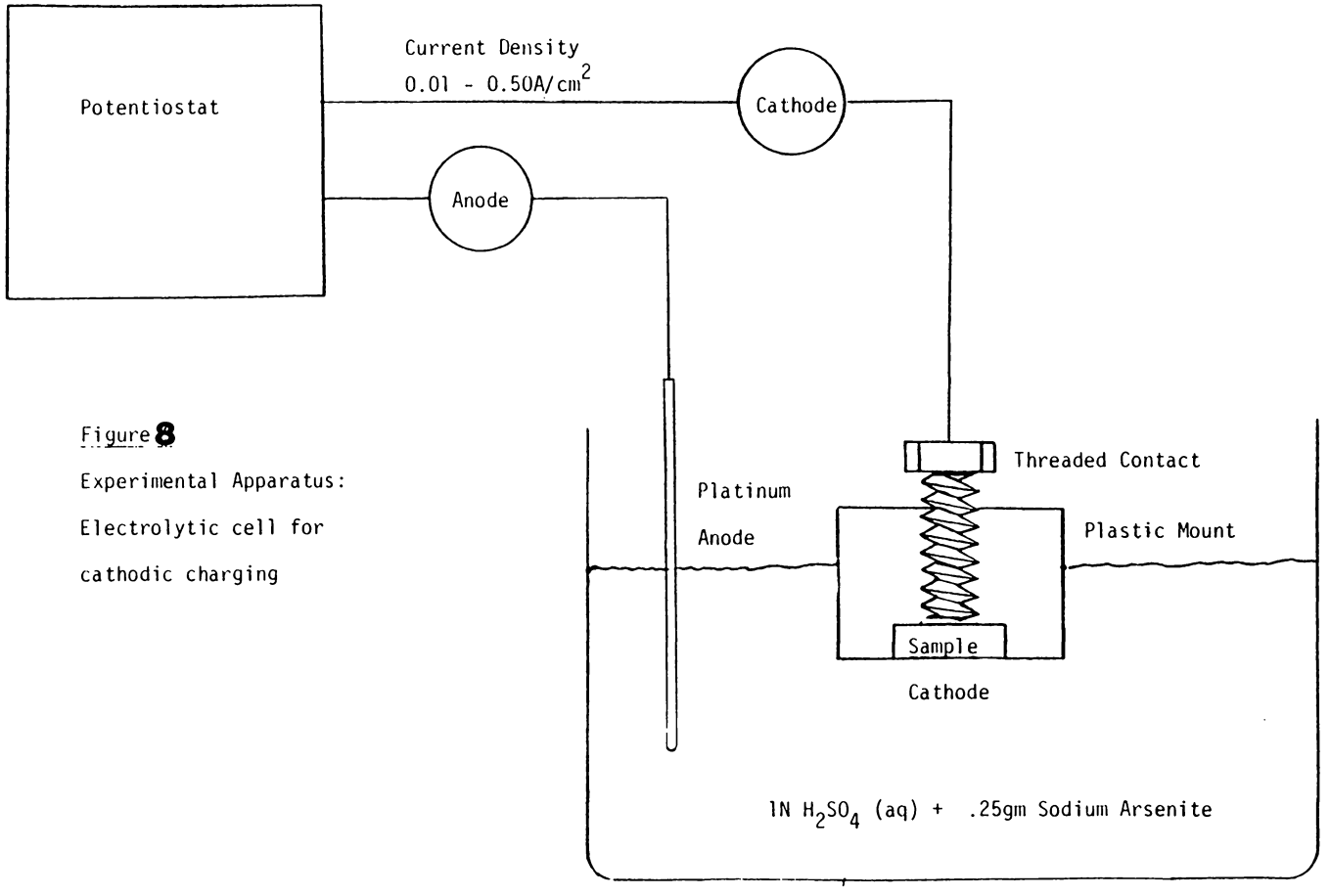

Figure 8

Experimental Apparatus:
Electrolytic cell for
cathodic charging

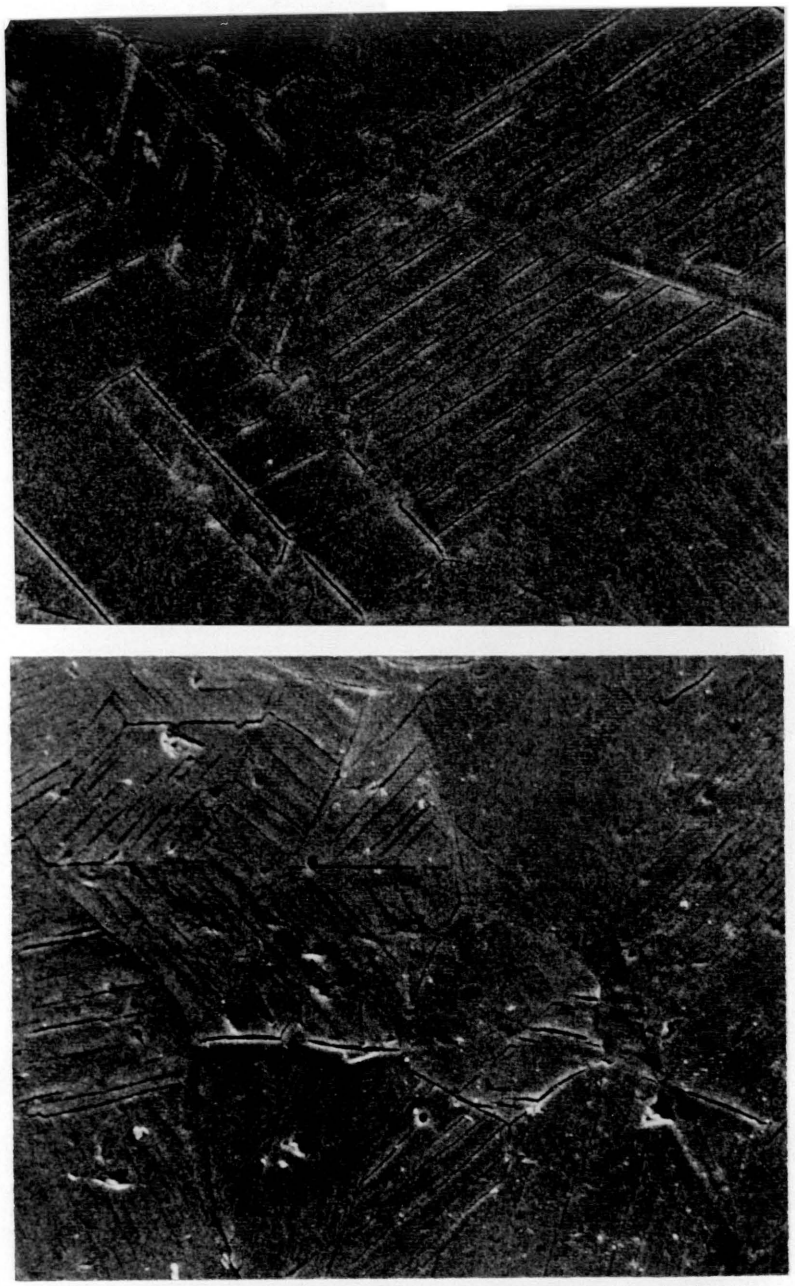

Figure 9. Scanning Electron Micrographs of A.HERF 316 Stainless Steel samples which have been cathodically charged for 2 hours at 0.5A/cm^2

accentuate surface cracking, and confirm that this phenomenon is occurring.

The effect of outgassing time, charging time, and current density, on the surface cracking susceptibility of different sample microstructures was determined utilizing these micrographs. The variables held contant during this experimental investigation were: electrolyte temperature (20°C), electrolyte integrity and composition, aging time, sample surface finish (0.05microns), and cell anode material (platinum). The platinum anode was also electrolytically cleaned between experiments.

After charging, samples were lightly vibration polished for 15 seconds in 0.05 micron alumina, to remove surface stains induced by charging experiments. Photomicrographs were taken using the Reichert MEF2 light microscope, at magnifications varying from 200X to 800X, and prints were developed from black and white Kodak technical print 35mm negatives on high contrast Kodak paper. Electron micrographs of some samples were taken on the Jelco JSM-2 Scanning Electron Microscope at magnifications of 1000X. These micrographs were used to supplement the information contained in the photomicrographs, and support the conclusions developed in this report.

IV EXPERIMENTAL RESULTS AND DISCUSSION

Previous work has established the susceptibility of metals and alloys to hydrogen induced surface cracking, caused by the ingress of electrolytic hydrogen, into samples which have no externally applied stress. While work has been done to investigate the fractographic characteristics of cathodically charged 316 stainless steel and Co- based ZIMALOY implant materials, a microstructural basis for the surface cracking characteristics has not been established.

An understanding of the relative susceptibilities of the various microstructural features to hydrogen embrittlement, would provide a method for improving the reliability of metals used in hydrogen environments. Both 316 stainless steel and ZIMALOY are known to be susceptible to adverse hydrogen effects. Changes in processing, such as HERFing, annealing, and sensitizing, would produce microstructural features which are affected to different degrees by electrolytic hydrogen charging. Materials which must be used in hydrogenous environments could then be processed in a manner which would produce the most hydrogen compatible microstructure.

The purpose of this investigation therefore, is to determine the relative susceptibility of different microstructural features, and suggest techniques for the

use of microstructure in controlling hydrogen induced cracking.

In order to determine the microstructural justification for the observed hydrogen effects on 316 stainless steel and ZIMALOY, it was necessary to experimentally observe surface cracking at the various microstructural features. Photomicrographs and scanning electron micrographs were taken for this purpose. To insure that only hydrogen effects were responsible for the observed cracking in the different microstructures tested, various charging techniques were used before a standard charging condition was developed. Once this standard condition was adequately demonstrated, the isolated effects of current density and charging time were determined, and a microstructural methodology for controlling surface cracking in 316 stainless steel and ZIMALOY was established.

A. Isolating Hydrogen Exposure Effects

Many experimental variables affect the characteristics of hydrogen induced surface cracking. Comparison of the relative compatibility of metals and alloys is often difficult because of differences in test conditions. For cathodic charging studies these variables include:[44 48]

specimen surface finish; electrolyte composition and age; test temperature; aging time; and hydrogen exposure history. In this investigation, the effects of hydrogen exposure were determined by holding all variables except charging time and current density constant.

The individual control of several of these test variables has been previously discussed: test temperature (section III. C. page 39); electrolyte composition and integrity (section III. C. page 39); and sample surface finish (section III. A. page 23). The effects of aging time however, are particular to a given experiment, as well as sample composition and processing history. The proper aging times for the various samples used in this investigation were therefore determined experimentally.

After a sample has been cathodically charged, the time that it is allowed to outgas (age) will affect the extent of observed surface cracking.[8 14 15 44 48] It is therefore necessary to determine the time required for surface cracking to reach an equilibrium condition, after which no further cracking occurs. Figure 10 is a set of photomicrographs of the identical surface region of a typically charged sample, which has been subsequently aged at time of 0 and 6 hours, respectively. Comparisons of these figures demonstrates the dependence of of surface

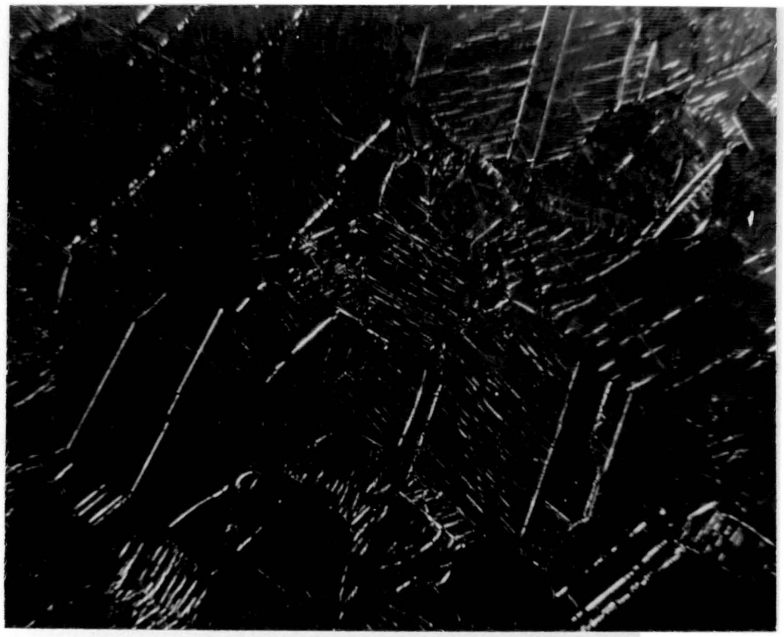

a. aging time = 0 hours (400X)

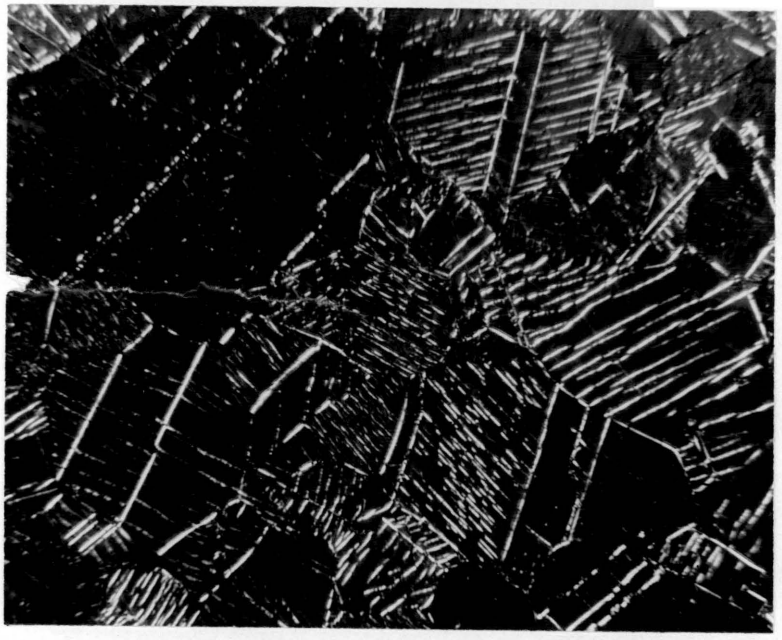

b. aging time = 6 hours (400X)

Figure 10 Photomicrographs showing the effects of aging time on annealed HERF 316 stainless steel samples that have been cathodically charged for 2 hours at a current density of (0.05 amps/cm^2)

cracking on aging time, and concurs with the results of other studies which demonstrated similar aging effects for 316 stainless steel.[8 14] Other tests also demonstrated that no additional surface cracks were observed after aging stainless steel and ZIMALOY samples approximately 4 and 10 hours , respectively. To insure that no further cracking would occur. Photomicrographs presented in this report, unless otherwise noted, were taken at aging times greater than 12 hours for both 316 stainless steel and ZIMALOY samples. This aging time is sufficient to eliminate the influence of outgassing on experimental observations, and insure that standard cracking severity comparisons could be made between micrographs.

B. Microstructural Effects of Cathodic Charging

The occurrence of surface cracking due to electrolytic hydrogen exposure is discussed in the literature for a wide variety of materials,[44-51] including 316 stainless steel.[8 14] A microstructural basis for the characteristics of this surface cracking has not been extensively developed. Such a developement is important if we are to understand why changes in processing have been observed to affect the hydrogen compatibility of materals in both gaseous and

electrolytic hydrogen environments.[10 12 13 52 54 58] Since a correlation between hydrogen compatibility and processing for various compositionally different alloys exists, it is possible that microstructural similarity between alloys is responsible for the similar behaviour in hydrogeneous environments. These observations led one investigator to conclude that "if we are to proceed further with our understanding of hydrogen cracking ..., we must obtain a detailed picture of hydrogen induced crack propagation paths ...".[51] The results of this investigation will assess this microstructural picture, and will facilitate an understanding of how changes in processing can be utilized to improve the hydrogen compatibility of 316 stainless steel and ZIMALOY orthopedic implant materials, and should be applicable to other materials used in hydrogeneous environments.

The samples used in this investigation, regardless of composition or method of processing, were simply cathodically charged to produce surface cracking. The characteristics of the resulting cracks however, varied extensively depending on how the sample was processed (see Figures 11-15). The cracking in all samples however, occurs almost exclusively along specific microstructural features, which are characteristic of the method of sample processing.

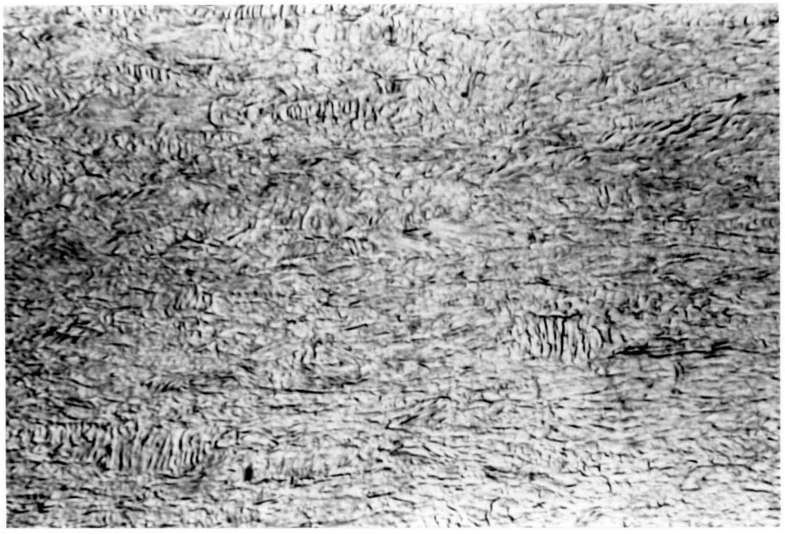

Figure 11 Photomicrograph of HERF 316 stainless steel cathodically charged (0.05 amps/cm^2) continuously for 2 hours (200X)

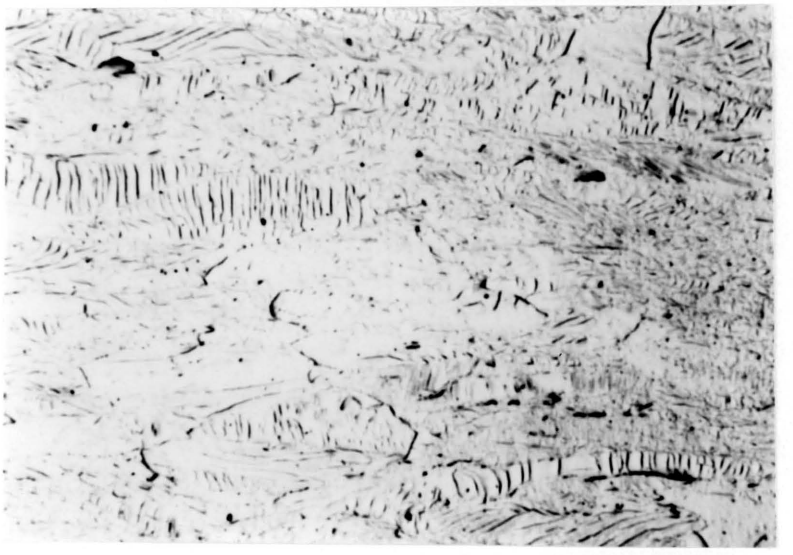

Figure 12 Photomicrograph of S.HERF 316 stainless steel cathodically charged (0.05 amps/cm^2) continuously for 2 hours (200X)

Figure 13 Photomicrograph of A.HERF 316 stainless steel cathodically charged (0.05 amps/cm^2) continuously for 2 hours (200X)

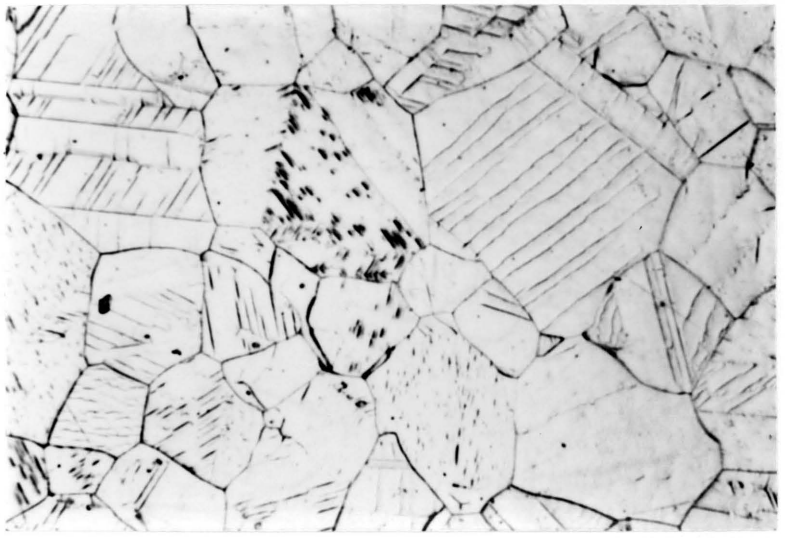

Figure 14 Photomicrograph of S.A.HERF 316 stainless steel cathodically charged (0.05 amps/cm^2) continuously for 2 hours (200X)

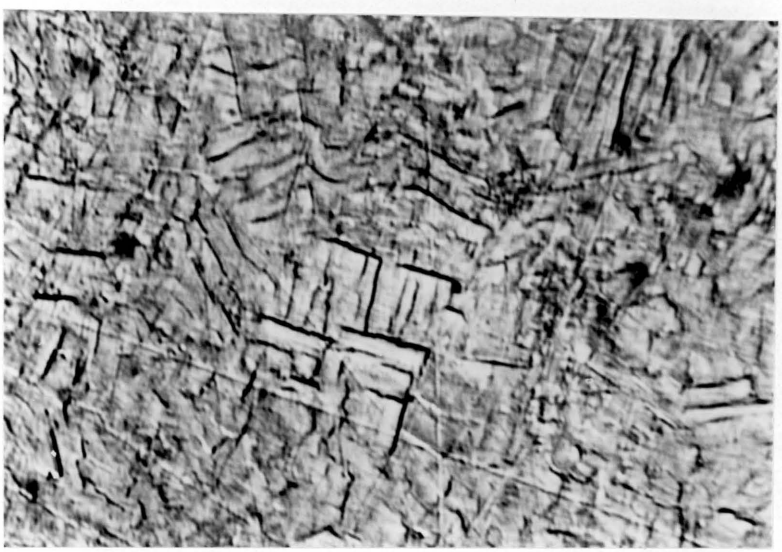

Figure 15 Photomicrograph of H.I.P. ZIMALOY orthopedic implant material cathodically charged (0.05 amps/cm^2) continuously for 12 hours (200X)

This is particularly evident if photomicrographs taken after cathodic charging are compared to those taken prior to charging. For instance, in HERF (see Figure 11) and S.HERF (see Figure 12) samples, the dislocation dense slip bands are most extensively cracked, as are the twin boundaries in A.HERF (see Figure 13) and H.I.P. ZIMALOY (see Figure 15) samples. Photomicrographs taken prior to cathodic charging illustrate the existence of all these feature in etched samples (see Figures 1-4,6,7). It is important to note, that while these photomicrographs show easily deformable grain boundary structure in all samples prior to charging however, only samples which were sensitized (S.HERF and S.A.HERF) showed any significant amount of intergranular cracking (see Figures 12 and 14, respectively).

It is evident, therefore, that while all samples cracked, different microstructural features cracked depending on how the material was processed: in some samples only one specific microstructural feature cracked; while in other samples several microstructural features cracked. These observations support the contention that different microstructural features require varying degrees of hydrogen ingress and subsequent lattice strain energy, to become preferred regions of crack initiation and propagation. For instance, if not enough hydrogen

absorption occurs during charging, no cracking will occur, while at high hydrogen contents numerous features crack. Hydrogen contents, and therefore cathodic current densities in the intermediate range, produced internal conditions adequate to induce cracking only along the most susceptible regions. Therefore, through variations in cathodic charging current density, which are known to produce varying amounts of hydrogen absorption, subsequent changes in the extent of hydrogen damage can be determined, and the relative susceptibilities of specific microstructural features to hydrogen embrittlement, can be established.

C. Effects of Current Density on Microstructural Compatibility

Variations in current density cause changes in the amount of hydrogen that is absorbed into the surface of a sample during charging. High current densities cause large quantities of hydrogen to be absorbed, and subsequently large lattice distortions result because of the positive partial molar volume of hydrogen in solution. This causes the sample surface to expand during charging, and substantial tensile forces to be developed at the surface during outgassing (aging) as the sample surface tries to

contract. These stresses cause a tendency of cracking along the sample surface. Low current densities however, cause only mild tensile forces to develop during aging.

The strain energy produced by hydrogen absorption and outgassing at low current densities is only sufficient to produce cracking along the most susceptible paths within the microstructure. Testing at high current densities however, provides absorbed hydrogen concentrations and lattice strains large enough to cause the cracking of other microstructural features. The specific features that crack are therefore dependent on the charging current density, because different features will require different amounts of absorbed hydrogen before cracking is initiated. The least susceptible microstructural features will require high current densities to induce cracking, while the most susceptible paths will crack at low current densities.

Increases in the current density have been demonstrated to significantly increase the extent of detrimental surface cracking.[44 48] The results of samples tested in this investigation support that result and showed that increases in current density cause an increase in the severity of surface cracking, and changed the cracking characteristics. This current density effect is shown in Figures 16 - 21, which show photomicrographs of the different samples,

charged at cathodic current densities of 0.01 amps/cm^2 (low) and 0.50 amps/cm^2 (high). The low current density was established because 0.01 amps/cm^2 was just sufficient to induce surface cracking in all samples tested, primarily along the most susceptible microstructural features, after reasonable charging times. The high current density of 0.50 amps/cm^2 was found to be of sufficient magnitude to induce cracking in at least two microstructural features in 316 stainless steel and H.I.P. ZIMALOY samples.

The samples of HERF, S.HERF, A.HERF, and S.A.HERF 316 stainless steels and H.I.P. ZIMALOY, displayed cracking characteristics which were strongly dependent on how they were processed (see Figures 16-21) It is therefore beneficial to compare photomicrographs taken prior to cathodic charging (see Figures 1-4,6,7), with those taken after cathodic charging. This will aid in recognizing which microstructural features have cracked, so that conclusions on the relative susceptibility of different microstructural features to hydrogen induced cracking can be established.

Cracking in the HERF 316 stainless steel, shown in Figure 16, illustrates that cracking is microstructurally orientated, and that the observed cracking characteristics change as the current density is increased. The photomicrograph taken at 0.01 amps/cm^2, shows that at low

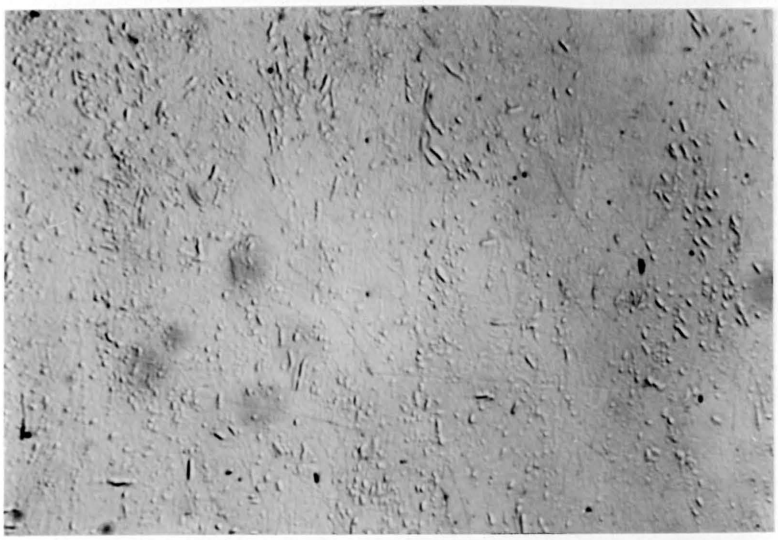

a. Current Density = (0.01 amps/cm^2) 200X

b. Current Density = (0.50 amps/cm^2) 1000X (S.E.M.)

Figure 16 Photomicrographs showing the effects of current density on HERF 316 stainless steel samples which have been cathodically charged for 2 hours at the specified current density

a. Current Density = (0.01 amps/cm^2) 200X

b. Current Density = (0.50 amps/cm^2) 2000X (S.E.M.)

Figure 17 Photomicrographs showing the effects of current density on S.HERF 316 stainless steel samples which have been cathodically charged for 2 hours at the specified current density

a. Current Density = (0.01 amps/cm^2) 400X

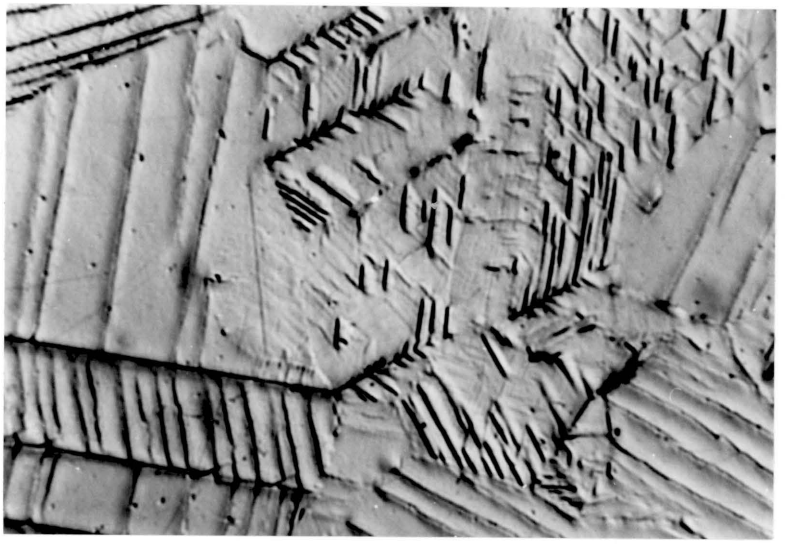

b. Current Density = (0.50 amps/cm^2) 800X

Figure 18 Photomicrographs showing the effects of current density on A.HERF 316 stainless steel samples which have been cathodically charged for 2 hours at the specified current density

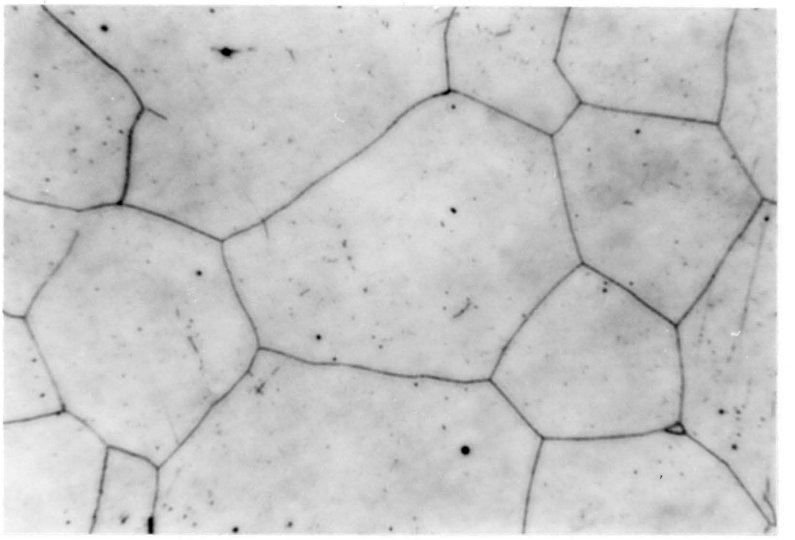

a. Current Density = (0.01 amps/cm^2) 400X

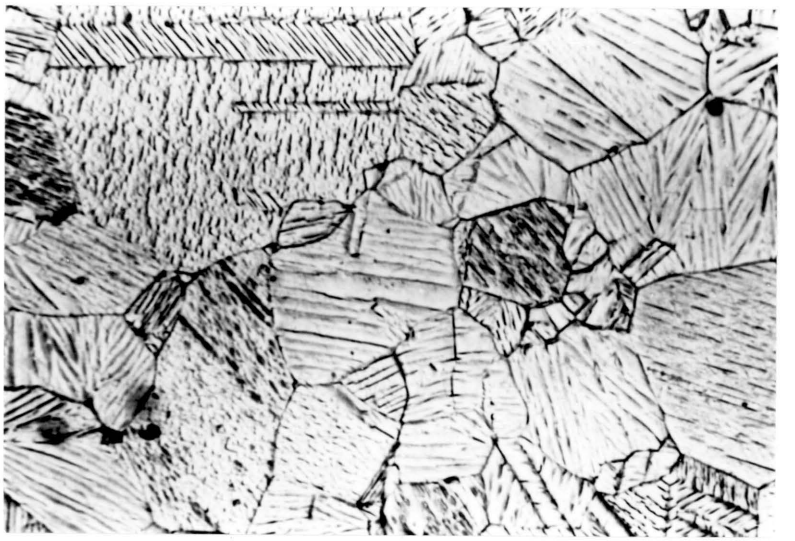

b. Current Density = (0.50 amps/cm^2) 200X

Figure 19 Photomicrographs showing the effects of current density on S.A.HERF 316 stainless steel samples which have been cathodically charged for 2 hours at the specified current density

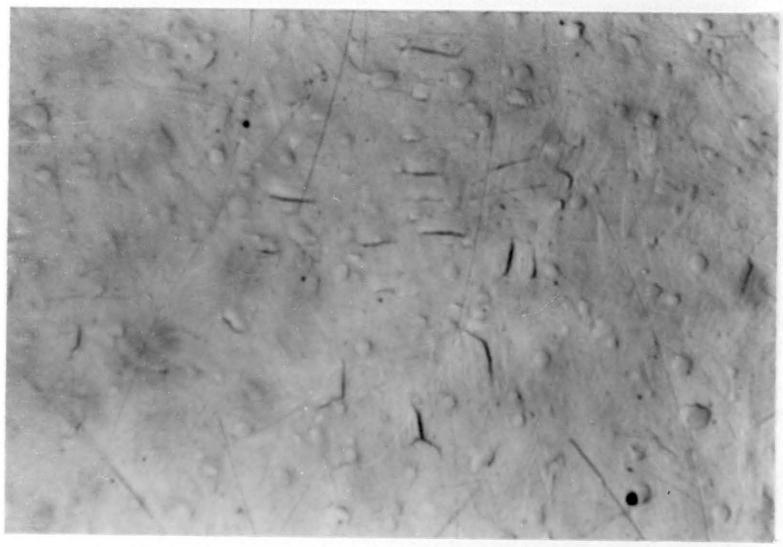

a. Current Density = (0.01 amps/cm^2) 400X

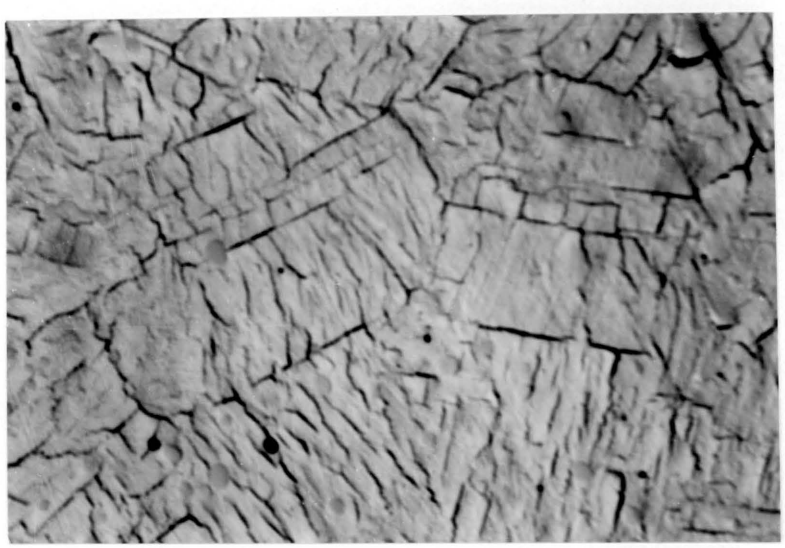

b. Current Density = (0.50 amps/cm^2) 400X

Figure 20 Photomicrographs showing the effects of current density on H.I.P. ZIMALOY implant samples which have been cathodically charged for 12 hours at the specified current density

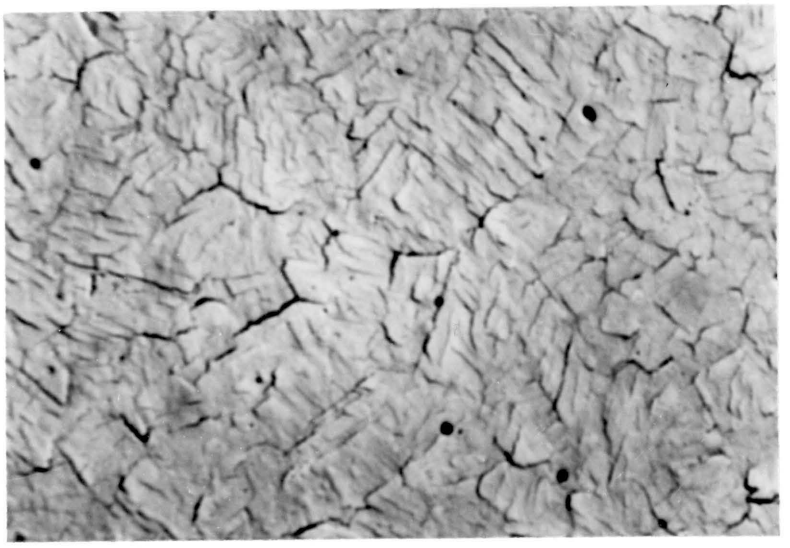

a. Current Density = (0.50 amps/cm^2) 400X

Figure 21 Photomicrographs showing the effects of current density on H.I.P. ZIMALOY implant samples which have been cathodically charged for 12 hours at the specified current density

current densities slip band cracking is evident, and some hydrogen induced surface roughness has also occurred (see Figure 16 a.). This cracking is very fine in nature, due at least in part to the fine grain structure, characteristic of HERFed materials.

As expected, the amount of observed cracking increases as the current density is increased to 0.50 amps/cm^2 (see Figure 16 b.). At this high current density, cracking has become extended along slip bands, and random cracking is evident throughout the matrix. These observations show that in HERF material, slip bands crack most easily, and as current density increases, random matrix cracking occurs rather than grain boundary parting. The grain boundary structure in HERF material, is therefore the least susceptible to cracking. The occurrence of extensive matrix cracking in conjunction with slip band cracking at high current densities, however, suggest that while cracking at low current densities is not extensive or connected, high current densities decrease the integrity of HERFed materials excessively by forming large scale, connected cracks. These observations may explain the results of other investigations, which showed that the hydrogen compatibility of HERFed materials decreased markedly in high pressure hydrogen,[11] [12] even though good compatibility was demonstrated at low hydrogen pressures.

S.HERF materials behave similar to HERF materials, in that cracking along slip bands is prevalent at both low and high current densities, the latter being more extensive (see Figure 17). Photomicrographs taken after charging at 0.01 amps/cm^2, show that for the most part, slip band cracking has occurred with only limited surface roughness (see Figure 17 a.). In comparison to non-sensitized HERF (see Figure 16 a.), slip band cracks in S.HERF samples are longer and more numerous, while less general surface roughness occurs.

The matrix cracks in HERF samples at high current densities were detrimental because of their tendency to join, but the cracking along the grain boundaries of S.HERF sample (see Figure 16 a.) is much worse, in that it produces an extensive network of extended cracks. This continuous cracking after charging at 0.05 amps/cm^2 suggests that sensitization treatments decrease the compatibility of HERFed 316 stainless steel with hydrogeneous environments, and should be avoided if exposure to hydrogen is anticipated.

A.HERF and S.A.HERF samples are microstructurally different than HERFed materials, in that they contain recrystallized grains free of the dislocation dense slip bands. Comparisons between photomicrographs taken prior to

charging (see Figures 3 and 4), and those taken after charging (see Figures 18 and 19), show that cracking still occurs along specific microstructural features which are characteristic of the method of thermomechanical processing.

The photomicrograph of the A.HERF sample charged at 0.01amps/cm^2 (see Figure 18 a.), shows that cracking is most extensive along twin boundaries, while slip planes also appear to crack easily. Comparison to HERFed samples charged at low current densities, however, show that both twins and slip planes cracked easily in annealed samples, while only small amounts of slip band cracking occurred in HERFed samples. These results may explain the results of other investigations, which showed that HERFed materials are more compatible in low pressure hydrogen environments than are annealed materials of the same chemical composition.[13] [52-54 58]

As the current density is increased the grain boundary and matrix retain their integrety, while cracks already initiated along slip planes and twins become extended. Therefore, while cracks become increasingly longer during increasingly severe chargings, the detrimental nature of cracking does not change appreciably. Because, without interconnecting features such as grain boundary or random matrix cracking, the hydrogen induced cracks do not join to

form a continuously cracked microstructure. These results suggest an explanation for the observation that in very high pressure hydrogen environments, annealed materials perform better than HERFed materials, while at low current densities the opposite is true.

The annealed and sensitized samples contain the same microstructural features as A.HERF samples, however,sensitization has caused the chemical composition along grain boundaries and other structures to change. Photomicrographs taken after cathodic charging show that surface cracks along grain boundaries is extensive, at both high and low current densities (see Figure 19.). This results in a microstructure which is extensively cracked at a current density of only 0.01 amps/cm^2 (see Figure 19 a.). The continuous nature of this cracking, as well as the quantity of cracking, make S.A.HERF samples the most adversely affected stainless steel tested.

As current density is increased, the concentration of absorbed hydrogen in the S.A.HERF becomes sufficient to cause cracks along twin boundaries and slip planes to initiate, and extended transgranularly. This cracking in conjunction with already existing cracks along grain boundaries, could cause an extensive decrease in the integrity of this material in environments where high

pressure hydrogen is present. The detrimental compatibility of S.A.HERF observed in this investigation could explain the decreased hydrogen compatibility of sensitized materials, noted in the literature;[46 50 51 54] noted in the literature;[46 50 51 54 62-66] this decreased compatibility is the result of the extensive susceptibility of most of the microstructural features present in sensitized materials.

The H.I.P. ZIMALOY used in this investigation has a very fine microstructure (see Figures 6,7), which characteristically contains twin boundaries primarily in the larger grains of the duplex grain structure. This duplex structure (see Figure 7), is characteristic of materials that have been H.I.Ped. The H.I.P. ZIMALOY used in this investigation therefore, has relatively large grain size in the medial region, while the exterior region of the implant device is small grained. Therefore, cracking in the small grained region will be responsible for the in service compatibility of materials that are H.I.Ped, such as the orthopedic implants stem sections studied in this investigation. The photomicrograph taken at a current density of 0.01 amps/cm^2 (see Figure 20 a.), illustrates that very little cracking occurs at this current density, in the small grained region of the sample. The relative compatibility of this material is therefore the best of any

material tested. The cracking shown in Figure 20 a., however, does demonstrate that twins are the most easily cracked microstructural feature in H.I.P. ZIMALOY, even though such cracking required larger concentrations of absorbed hydrogen.

As in all other samples tested, as the current density is increased the subsequent amount of surface damage in H.I.P. ZIMALOY samples increased. The photomicrographs in Figures 26 b. and 27, show the effect of high current density on the large grained medial region, and small grained surface region of H.I.P. ZIMALOY samples, respectively. The large grained sample is more severely cracked especially along twin boundaries and what appear to be slip planes. The small grained sample is cracked randomly for the most part. It is apparent that the large grained structure is much more extensively cracked due to the electrolytic hydrogen exposure, than was the small grained region. This result may explain data in the literature which suggests that decreases in grain size increase the compatibility of materials tested in hydrogen environments.[54] [56]

The results of these current density tests demonstrate that increases in current density cause an increase in the

extent of hydrogen induced surface damage. For the different materials tested, the relative susceptibility of the different microstructural features has been evaluated. The correlation between the results in this investigation, and data in the literature, strongly suggest that the relative compatibility of materials manufactured utilizing different processing techniques, is due to the inherent susceptibility of certain microstructural features, to hydrogen induced cracking. This suggests that changes in processing, which change microstructure, may be utilized as a method of increasing the hydrogen compatibility of materials. Before this can be adequately discussed however, a more accurate assessment of microstructural susceptibility must be made through analyzing the effects of charging time on hydrogen induced surface cracking. This will be accomplished by analyzing the effects of charging time at low current densities. At low current densities, the most susceptible features to hydrogen damage can be identified. And, by identifying which features crack easiest, processing techniques can be utilized which avoid their formation, and subsequently increase the compatibility of materials used in hydrogen environments.

D. Effects of Charging Time on Microstructural Compatibility

While the results of current density tests established a rough hierarchy of the relative susceptibility of the different microstructural features in H.I.P. ZIMALOY and 316 stainless steel samples to hydrogen induced surface cracking, in several of the current density tests this demarcation was not clearly evident. For instance, in annealed and sensitized annealed samples more than one microstructural feature cracked extensively at low current densities. In order to differentiate between these subtle differences in susceptibility, changes in charging time were utilized.

Data in the literature demonstrates that increases in charging time as well as current density affect the extent of surface cracking.[44 48] However, even though increases in both these charging variables result in increases in surface cracking, they affect the surface cracking characteristics of the sample differently. Increases in current density and charging time both increase the total amount of absorbed hydrogen; however, the amount of hydrogen absorption at the

sample surface is controlled by the equilibrium that exists between H(ads) and H(abs). The amount of hydrogen that is adsorbed onto the sample is controlled by the current density, and increases in magnitude as the current density is increased. Therefore, changes in the length of charging time have no affect on H(ads), and only affect the amount of hydrogen that can be absorbed at equilibrium, and the surface hydrogen concentration does not change. Increases in time therefore increase the total amount of hydrogen absorption by allowing additional time for diffusion to occur. This results in only moderate increases in hydrogen absorption, because of the low hydrogen diffusivity at room temperature.

Holzworth and Louthan established that changes in charging time caused variations in the extent of subsequent surface damage.[44] Photomicrographs in Figures 22 - 26 show the effects of charging time on the various samples tested in this investigation, and illustrate that increases in charging time cause subsequent increases in the amount of surface cracking. But at the low current densities utilized in this study, charging time effects cause only subtle changes in hydrogen absorption, and subsequently only the most susceptible features are cracked. The most susceptible microstructural features crack at the shortest charging

a. Charging Time = 1 Hour (200X)

b. Charging Time = 6 Hours (200X)

Figure 22 Photomicrographs showing the effects of charging time on A.HERF 316 stainless steel samples which have been cathodically charged at a current density of (0.01 amps/cm^2) for the specified time

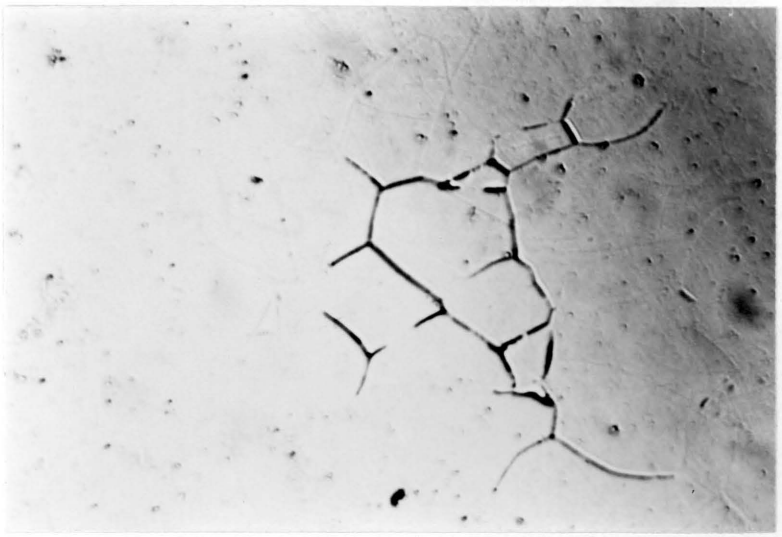

a. Charging Time = 1 Hour (200X)

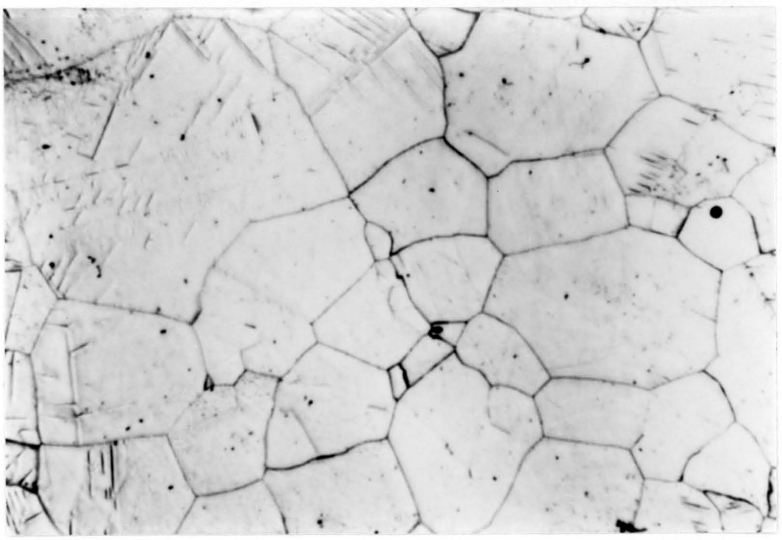

b. Charging Time = 6 Hours (200X)

Figure 23 Photomicrographs showing the effects of charging time on S.A.HERF 316 stainless steel samples which have been cathodically charged at a current density of (0.01 amps/cm^2) for the specified time

a. Charging Time = 6 Hours (200X)

Figure 24 Photomicrograph showing the effects of charging time on HERF 316 stainless steel samples which have been cathodically charged at a current density of (0.01 amps/cm^2) for 6 hours

b. Charging Time = 6 Hours (200X)

Figure 25 Photomicrograph showing the effects of charging time on S.HERF 316 stainless steel samples which have been cathodically charged at a current density of (0.01 amps/cm^2) for 6 hours

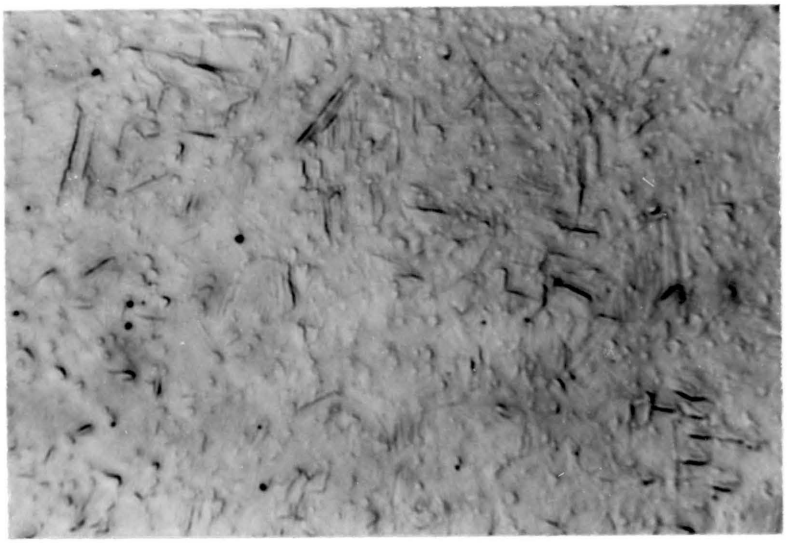

a. Charging Time = 24 Hours (400X)

Figure 26 Photomicrograph showing the effects of charging time on H.I.P. ZIMALOY implant samples which have been cathodically charged at a current density of (0.01 amps/cm^2) for 24 hours

times, while those feature nearly as susceptible, have cracking occur at slightly longer charging times. Thus, the effects of charging time at low current densities allows the relative susceptibility of microstructural features to be clearly identified.

The A.HERF and S.A.HERF samples experienced the most severe cracking of any samples tested (see Figures 23 and 24, respectively). While other samples required at least two hours for sufficient hydrogen absorpbtion and subsequent cracking to occur, only 1 hour was required for surface cracks to become apparent in A.HERF and S.A.HERF samples. In both cases, cracking was predominatly along a specific microstructural features: in A.HERF, twins cracked easiest (see Figure 22 a.), while in S.A.HERF samples the sensitized grain boundaries cracked first (see Figure 23 a.). In both these samples however, other features were cracked to a lesser degree after only one hour of charging. A twin boundary which is just beginning to crack is seen in the S.A.HERF sample (see Figure 23 a.), while slip plane cracking is apparent in the A.HERF sample (see Figure 22a.). The increase in charging time causes a small increase in absorbed hydrogen content and produces sufficient stress to cause cracking in other features which are only slightly less susceptible to hydrogen embrittlement. It is therefore

rationalized that while twins appear to be the most susceptible to cracking in annealed samples, the relative ease with which slip planes cracks, suggests that they are nearly as susceptible as twin boundaries.

In the HERF (see Figure 24), S.HERF (see Figure 25), and H.I.P. ZIMALOY samples (see Figure 26), however, the increase in hydrogen absorption is sufficient to only increase the number of cracks, located primarily along the slip bands in HERF and S.HERF samples, and the twin boundaries in H.I.P. Zimaloy. Also the increase in charging time caused the extension of already existing cracks. The other microstructural features which did crack at higher current densities, did not achieve sufficient hydrogen ingress during charging to initiate hydrogen induced damage. Therefore, slip bands are clearly the most susceptible feature in HERFed materials, as are twins in H.I.P. ZIMALOY. Other features, such as grain boundaries, are substantially less susceptible to hydrogen embrittlement.

The results of these charging time effects, in conjunction with current density effects, suggest that sensitized materials are the most susceptible to surface cracking. Also, results suggest that in non-sensitized materials, twins crack most readily if they are present in the microstructure. Similarly, the cracking of slip planes in these samples is also extensive.

Since orthopedic implant applications involve exposure to low current densities for extended periods of time, and subsequent hydrogen absorption can cause surface cracks which degrade the fatigue resistence of implanted materials, consideration should be given to the results of this investigation. Only the most susceptible microstructural features will be degraded due to in vivo exposure. Therefore, A.HERF and S.A.HERF samples should be avoided due to the presence of microstructural features which could crack at the low cathodic charging current densities generated in the body. For implant application it would be suggested that H.I.P. ZIMALOY be used in preference to stainless steel whenever possible, and that when stainless steel is required it should be used in the HERF condition.

E. Effects of Microstructure on Hydrogen Compatibility

The results presented in this thesis illustrate the microstructural dependence of surface cracking which occurs in materials to resulting from cathodic charging of hydrogen. While cracking is observed in all samples investigated, the characteristics of the observed cracking varied extensively between samples, due to differences in processing technique. Correspondingly, the relative

compatibility of samples to surface cracking varied. While the possible effects of microstructure could influence the compatibility of surgical implants, the applicability of microstructure as a means of controlling the extent of hydrogen damage, can be applied to a wide variety of applications.

The compatibility of a sample is assessed by measuring the quantity of surface cracks, and the characteristics of these cracks. For the most part, microstructures that promote many small regions of randomly dispersed cracks, are preferred over microstructures that allow a small number of regions of extensive cracking in an interconnected or continuous manner. The detrimental nature of this type of cracking has already been discussed in reference to cracking that occurs at high current densities, in materials which have been sensitized. Also, compatibility would require that the processing technique be such that it produces microstructural features that are minimally susceptible to hydrogen effects. Since we have already demonstrated the dependence of surface cracking on microstructure, the general ranking of microstructural susceptibility which was established this could provide a method for increasing hydrogen compatibility by minimizing the existence of susceptible features.

Probably the most important observation in this investigation, is that H.I.P. ZIMALOY is the most compatible material of any tested. Not only did cracking require extended charging times, but cracks that did occur were less extended and fewer in number, than in any stainless steel. While this alloy is compositionally different from the stainless steel alloys, microstructural similarities can still be utilized for determining the compatibility of certain microstructural features,

In all samples tested in this investigation, twins were found to crack easily, while only in sensitized samples did boundary cracking occur. However,while the ZIMALOY microstructure contains twins, it was by far the least affected sample tested, requiring extended periods of time at a given current density to induce cracking. It must be remembered however, that when comparing microstructural effects in H.I.P. ZIMALOY and 316 stainless steels, certain materials are inherently more compatible with cathodic hydrogen than are other materials, due to compositional effects. A similar dependence of composition on hydrogen compatibility has been shown extensively in the literature.[10 13 46 52 54] This investigation however, is not concerned with identfying the effects of composition, but rather in demonstrating that certain microstructures are

inherently more susceptible to cracking than others, regardless of alloy type or chemical composition. Once this has been demonstrated, processing techniques can be utilized to produce a material which has a greater relative hydrogen compatibility, than the same material processed in a different manner.

The H.I.P. process produces a microstructure which contains both twins and fine grains of various size. It was noted that the first features to crack in ZIMALOY were the twins with some slip plane cracking was observed at higher current density in the large grained sample. Similarly, twins were also the most susceptible microstructural feature in A.HERF samples, and cracked extensively in S.A.HERF samples as well. This suggest that twins boundaries are the microstructural feature most susceptible to hydrogen induced cracking, in these fcc alloys. Therefore avoiding twins by HERFing could be used to improve compatibility in hydrogeneous environments, where low pressure hydrogen exposure are expected.

It was also note that in the regions of decreased grain size, the H.I.P. material was least affected by hydrogen. HERF materials, which also have a characteristically fine grain size, were also shown to have an increased overall compatibility with hydrogen. While the compatibility of

HERFed materials is at least in part due to a lack of twins, the fact that in all non-sensitized samples grain boundary cracking did not occur, suggests that grain boundaries are a hydrogen compatible microstructural feature until very high hydrogen contents are achieved. The possible beneficial effect of reducing the grain size is noted in the literature,[44] [54] and cold working, which produces a dislocation dense sub-boundary structure, has also been found to improve hydrogen compatibility.[44] [53] The results of this investigation in conjunction with data in the literature, suggest a dependence of grain size on hydrogen compatibility. Processing techniques therefore, which produce fine grain structure, would also be expected to increase the resistance of a material to degradation by hydrogen environments.

While HERFed and H.I.P.microstructures were the least affected by electrolytic hydrogen absorption, sensitized treatments were found to have a detrimental affect on hydrogen compatibility. This investigation suggests that this lack of compatibility could be due to the relative ease with which sensitized boundaries cracked. Samples which were similarly processed, but not sensitized, showed no appreciable grain boundary cracking. In fact, random matrix cracking frequently occurred in preference to the cracking

of non-sensitized boundaries. While this is a chemical change, it produces detrimental changes in the susceptibility of a grain boundary to cracking, and should therefore be avoided.

The results of this investigation have therefore clearly demonstrated that hydrogen induced cracking occurs various microstructural features. Because certain microstructural features are more susceptible than others to surface cracking - regardless of composition -, processing changes can be utilized which produce the most compatible material for use in hydrogeneous environments. For orthopedic implant devices which are exposed to low current density in vivo hydrogen generation, when 316 stainless steel is required, non-sensitized HERFed materials should be used. However, if possible Co-based alloys are desired and H.I.P.ed materials, with their inherently fine grain size, should be used, rather than cast alloys which have a much larger grain size. For high hydrogen exposure, as in industrial applications, sensitized structures should be avoided, and HERFed or fine grained materials should be utilized.

V. CONCLUSIONS

The H.I.P. ZIMALOY and 316 stainless steel orthopedic implant materials studied in this investigtion are the preferred alloys for implant manufacture. These materials have shown good biocompatibility, maintaining both their chemical and mechanical integrity in the body. The advent of orthopedic implantation the children however, has extended the desired life expectancy of implants, and caused a corresponding increase in the occurrence of implant failure. Subsequently, an increase in the need to improve the compatibility of in vivo implant materials has resulted. Because hydrogen is generated in vivo, and has been shown to degrade the properties of both 316 stainless steel and ZIMALOY, changes in processing which change hydrogen biocompatibility could be utilized to improve implant life. Therefore, test were conducted to study the influence of processing, on the hydrogen compatibility of samples of 316 stainless steel and ZIMALOY exposed to cathodic hydrogen environments.

The results of these tests show that cathodic charging induced surface cracking in all 316 stainless steel and H.I.P. ZIMALOY samples tested. This hydrogen damage was found to increase as either the current density or charging

time was increased. These cracks were found to occur along specific microstructural features characteristic of the sample.

It was observed that twin boundaries crack most readily in non-sensitized samples, and that both grain boundaries and twin boundaries crack easily in sensitized structures. Therefore, these observations, coupled with the similarity between hydrogen embrittlement and failure of orthopedic implants, suggest that orthopedic applications should use H.I.P. ZIMALOY in preference to 316 stainless steel whenever possible, and that when the use of 316 stainless steel is unavoidable, HERFed parts should be used. The results also suggest that in the general application of materials in hydrogeneous environments, processing by H.I.P. or HERFing techniques, could be utilized as a means of improving hydrogen compatibility.

REFERENCES

1. E. J. Sutow, and S. R. Pollack, "The Biocompatibility of Certain Stainless Steels," CRC Series in Biocompatibility, CRC Press Inc., Boca Raton, Florida, 1981, p.45.

2. D. I. Bardos, "High Strength Co- Cr- Mo Alloy by Hot Isostatic Pressing of Powder," Biomat., Med. Dev., and Org., 1979, vol 7(1), p.73.

3. H. P. Chandler, et al., "Total Hip Replacement in Patients Younger Than 30 Years Old," Journal of Bone and Joint Surgery, Dec. 1981, vol 63-A, no. 9, p.1426.

4. D. F. Williams, "The Properties and Clinical uses of Cobalt- Chromium Alloys," CRC Series in Biocompatibility, CRC Press Inc., Boca Raton, Florida, 1981, p.99.

5. J. K. Wickstrom, "Surgical Implants - Their Mechanical and Environmental problems," Journal of Materials, 1966, vol 1, p.366.

6. D. L. Levine, and R. W. Staehle, "Crevice Corrosion in Orthopedic Implant Materials," Journal of Biomedical Materials Research, 1977, vol 11, p.553.

7. Brian Edwards, Thesis Report: "Hydrogen Embrittlement of an Orthopedic Implant Alloy," March 1981, Virginia Tech.

8. H. E. Hanninen, and T. Hakkarainen, "Fractographic Characteristics of a Hydrogen-Charged AISI 316 Type Austenitic Stainless Steel," Met. Trans., 1979, vol 10A, p.1196.

9. C. L. Briant, "Hydrogen Assisted Cracking of Austenitic Stainless Steels," Third International Conference on Hydrogen Effects on Metals, AIME, Moran Wyoming, Aug. 1980, p.565.

10. M. R. Louthan, Jr., G. R. Caskey, Jr., J. A. Donovan, and D. E. Rawl, Jr., "Hydrogen Embrittlement of Metals," Mater. Sci. Eng., 1972, vol 10, p.357.

11. A. J. West, and M. R. Louthan , Jr., "Dislocation Transport and Hydrogen Embrittlement," Met. Trans., 1979, vol 10A, p.1675.

12. M. R. Louthan, Jr., J. A. Donovan, and D. E. Rawl, Jr., Technical Note: "Effect of High Dislocation Density on Stress Corrosion Cracking and Hydrogen Embrittlement of Type 304L Stainless Steel," Corrosion, 1973, vol 29, no. 3, p.108.

13. M. W. Perra, "Sustained-Load Cracking of Austenitic Steels in Gaseous Hydrogen," Conference on Environmental Degradation of Engineering Materials, Sept. 1981, Virginia Tech., p.321.

14. D. Eliezer, "Hydrogen Assisted Cracking in Type 304L and 316L Stainless Steels," Third International Conference on Hydrogen in Metals, AIME, Moran Wyoming, Aug. 1980, p.565.

15. Hannu Hanninen, et al., "Effect of Aging on Embrittlement and Microstructures in Hydrogen Charged Thin Specimens of Austenitic Stainless Steel," Third International Conference on Hydrogen Effects in Metals, AIME, Moran Wyoming, Aug. 1980, p.575.

16. A. C. Fraker, and A. W. Ruff, "Metallic Surgical Implants: State of the Art," Journal of Metals, 1977, vol 29, p.22.

17. L. J. Harris, and R. R. Tarr, "Implant Failures in Orthopedic Surgery," Biomat., Med. Dev., and Org., 1979, vol 7(2), p.243.

18. I. LeMay, V. G. Lappi, and W. E. White, "Materials for Biomedical Application," Polymer Engineering and Science, Nov. 1975, vol 15., no. 11, p.789.

19. ASTM Designation F138-76, "Stainless Steel Bar and Wire for Surgical Implants (special quality)," Annual Book of ASTM Standards, Part 46, American Society for Testing and Materials, Philadelphia, 1978, p.504.

20. Zimmer Technical Report, "Micrograin H.I.P. ZIMALOY," (1978)

21. R. F. Hochman, and L. M. Taussig, "Improved Properties of Type 316L Stainless Steel Implants by Low-Temperature Stress Relief," Journal of Materials, 1966, vol 1, p.425.

22. N. D. Greene, and D. A. Jones, "Corrosion of Surgical Implants," Journal of Materials, 1966, vol 1, p.345.

23. E. Smethurst, "A New Stainless Steel Alloy for Surgical Implants Compared to 316 S12," Biomaterials, 1981, vol 2, p.119.

24. F. R. Morral, "Cobalt Alloys as Implant Materials," Journal of Materials, 1966, vol 1, p.384.

25. R. P. Frankenthal, and J. Kruger, Ed., "Passivity of Metals," The Electrochemical Society Inc., 1979, p.749.

26. J. P. Paul, "Forces Transmitted by Joints in the Human Body," Symposium on Lubrication and Wear in Living and Artificial Joints, Institute of Mechanical Engineers, London, 1967, p.8.

27. M. A. Imam, A. C. Fraker, and C. M. Gilmore, "Corrosion Fatigue of 316L Stainless Steel Co- Cr- Mo Alloy and ELI Ti-6Al-4V," ASTM Symposium on Corrosion and Degradation of Implanted Materials, STP 684, Kansas City, Md., May 1978, p.128.

28. W. B. Lisagor, "Corrosion and Fatigue of Surgical Implants," ASTM Standardization News, May 1975, p.20.

29. J. R. Cahoon, and H. W. Paxton, "Metallurgical Analysis of Failed Orthopedic Implants," Journal of Biomedical Materials Research, 1968, vol 2, p.1.

30. J. Charnley, "Fracture of Femoral Prostheses in Total Hip Replacement," Clinical Orthopedic Related Research, 1975, vol 111, p.105.

31. J. O. Galante, W. Rostoker, and J. M. Doyle, "Failed Femoral Stems in Total Hip Protheses," Journal of Bone and Joint Surgery, 1975, vol 57-A, p.230.

32. L. M. Patric, and K. R. Trosien, "Performance Studies of Hip Prostheses," Journal of Materials, 1966, vol 1, p.443.

33. K. R. Wheeler, and L. A. James, "Fatigue Behavior of Type 316 Stainless Steel Under Simulated Body Conditions," Journal of Biomedical Materials Research, vol 5, 1971, p.267.

34. A. B. Ferguson, P. G. Laing, and E. S. Hodge, "The Ionization of Metal Implants in Living Tissues," Journal of Bone and Joint Surgery, 1960, vol 42-A, p.77.

35. B. O. Weightman, J. M. Zarek, and A. C. Bingold, "Corrosion of a Cobalt- Chromium- Molybdenum Orthopaedic Implant," Medical and Biological Engineering, 1969, vol 7, p.679.

36. J. Cohen, "Performance and Failure in Performance of Surgical Implants in Orthopedic Surgery," Journal of Materials, 1966, vol 1, p.354.

37. W. W. Tennese, and J. R. Cahoon, "Sensitization Still a Problem in the Intergranular Corrosion of Stainless Steel Surgical Implants," Biomat., Med. Dev., and Org., 1973, vol 1(4), p.635.

38. H. Skinner, et al., Corrosion, Materials Characteristics and Local Tissue Reactions Associated With Osteosynthesis Devices, N.B.S. Special Publication, Proceedings from the Conference on Implant Retrival: Material and Biological Analysis, Gaithersburg, Md., May 1980, p.423.

39. J. Kruger, "Fundamental Aspects of the Corrosion of Matallic Implants," ASTM Symposium on Corrosion and Degradation of Implanted Materials, STP 684, Kansas City, Md., May 1978, p.107.

40. L. M. Taussig, "Examination of Orthopeadic Implant Failures," N.B.S. Special Publication, Proceedings from the Conference on Implant Retrival: Material and Biological Analysis, Gaithersburg, Md., May 1980, p.201.

41. S. A. Brown, K. Merritt, "Metal Allergy and Metallurgy," N.B.S. Special Publication, Proceedings from the Conference on Implant Retrival: Material and Biological Analysis, Gaithersburg, Md., May 1980, p.299.

42. J. T. Scales, Proceedings and Reports of Councils and Associates: "Examination of Implants Removed From Patients," Journal of Bone and Joint Surgery, 1971, vol 53-B, p.344.

43. J. Cohen, Abstracts of Proceedings of a Workshop on ; "Standardization of Metal Surgical Implants for Orthopedic Surgery," Journal of Biomedical Materials Research, 1970, vol 4, p.245.

44. M. L. Holzworth and M. R. Louthan, Jr., "Hydrogen-Induced Phase Transformations in Type 304L Stainless Steel," Corrosion, 1968, vol 24, p.110.

45. R. Liu, N. Narita, C. Altstetter, H. Birnbaum, and E. N. Pugh, "Studies of the Orientations of Fracture Surfaces Produced in Austenitic Stainless Steels By Stress Corrosion Cracking and Hydrogen Embrittlement," Met. Trans., 1980, vol 11A, p.1563.

46. Hannu Hanninen, Simo-Pekka Hannula, and Seppo Tahtinen, "Hydrogen Effects in Austenitic Stainless Steel," Conference on Environmental Degradation of Engineering Materials, Virginia Tech., Sept. 1981, p.347.

47. Hiedya Okada, Yuzo Hosoi,and Seizaburo Abe, Technical Note: "Formation of Cracks in Austenitic Stainless Steels Cathodically Charged with Hydrogen," Corrosion, 1970, vol 26, no. 7, p.183.

48. M. L. Holzworth, "Hydrogen Embrittlement of Type 304L Stainless Steel," Corrosion, 1969, vol 25, no. 3, p.107.

49. D. Eliezer, D. G. Chakrapani, C. J. Altstetter, and E. N. Pugh, "The Influence of Austenite Stability on the Hydrogen Embrittlement and Stress-Corrosion Cracking of Stainless Steel," Met. Trans., 1979, vol 10A, p.935.

50. C. L. Briant, "Hydrogen Assisted Cracking of Type 304 Stainless Steel," Met. Trans., vol 10A, 1979, p.181.

51. C. L. Briant, "A Fractographic Study of Hydrogen Assisted Cracking in Austenitic Stainless Steels," Conference on Environmental Degradation of Engineering Materials, Virginia Tech., Sept. 1981, p.335.

52. M. R. Louthan, Jr., D. E. Rawl, Jr., J. A. Donovan, and W. G. Holmes, "Hydrogen Embrittlement of Austenitic Stainless Steels," Technical Report, Savannah River Lab., South Carolina 29801

53. B. C. Odegard, and A. J. West, "On the Thermo-Mechanical Behavior and Hydrogen Compatibility Of 22-13-5 Stainless Steel," Mater. Sci. Eng., 1975, vol 19, p.261.

54. G. R. Caskey, "Hydrogen Damage in Stainless Steels," Conference on Environmental Degradation of Engineering Materials, Virginia Tech., Sept. 1981, p.283.

55. D. K. Collis, "Femoral Stem Failure in Total Hip Replacement," Journal of Bone and Joint Surgery, 1977, vol 59-A, p.1033.

56. C. L. Briant, and S. R. Banerji, "Intergranular Fracture in Steels: The Role of Grain Boundary Composition," International Metals Reviews, 1978, vol 2, p.164.

57 M. R. Louthan, Jr., J. A. Donovan, and D. E. Rawl, Jr., "Effect of High Dislocation Energy on Stress Corrosion Cracking and Hydrogen Embrittlement of Type 304L Stainless Steel," Corrosion, 1973, vol 29, p.108.

58. A. W. Thompson, "Ductility Losses in Austenitic Stainless Steels Caused by Hydrogen," Hydrogen in Metals, ASM, Metals Park, Ohio, 1974, p.91.

59. D. Hull, "Dislocations in Crystals," Pergamon Press, New York, 2nd Ed., 1979, p.122.

60. G. E. Dieter, "Mechanical Metallurgy," McGraw Hill Book Co., 2nd edition, 1976, p.127. 1977, p.1033.

61. R. Hill, "Physical Metallurgy," D. Van Nostrand Co., 2nd Edition, 1973, p.254.

62. H. E. Hanninen, "Influence of Metallurgical Variables on Environment Sensitive Cracking of Austenitic Alloys," International Metals Review, 1979, vol 24, p.85.

63. H. E. Hanninen, and T. Hakkarainen, "On the Effects of Alpha'-Martensite in Hydrogen Embrittlement of a Cathodically Charged AISI Type 304 Austenitic Stainless Steel," Corrosion, 1980, vol 36, p.47.

64. C. L. Briant, "Hydrogen Assisted Cracking of Sensitized 304 Stainless Steel," Met. Trans., 1978, vol 9A, p.731.

65. C. L. Briant, "A Mechanism for Intergranular Fracture in Type 304 Stainless Steel," Script. Met., 1978, vol 12, p.541.

66. C. L. Briant, "Hydrogen Assisted Cracking of Type 304 Stainless Steel," Met. trans., 1979, vol 10A, p.181.

The vita has been removed from the scanned document

Hydrogen Induced Surface Cracking of Two Orthopedic Implant Alloys

by

Ray C. Wasielewski

ABSTRACT

Electrolytic charging of hydrogen, at room temperature and in the absence of externally applied stress, induced surface cracking in 316 stainless steel and cobalt based ZIMALOY. Hot Isostatic Pressed (H.I.P.) ZIMALOY showed less susceptibility to surface cracking than 316 stainless steel samples. The susceptibility of 316 stainless steel to surface cracking was determined with samples in the High Energy Rate Forged (HERF), the sensitized, the annealed, and the annealed and sensitized conditions. Investigations showed that surface cracking typically occurred at specific microstructural features. Hence, the relative susceptibilities of twin boundaries, slip bands, grain boundaries, and heavily sensitized regions was established.

It was observed that twin boundaries crack most readily in non-sensitized samples, and that both grain

boundaries and twin boundaries crack easily in sensitized structures. These observations, coupled with the similarity between hydrogen embrittlement and failure of orthopedic implants, suggest that orthopedic applications should use H.I.P. ZIMALOY in preference to 316 stainless steel whenever possible, and that when the use of 316 stainless steel is unavoidable, HERFed parts should be used. Further investigations are recommended to better assess the hydrogen compatibility of sensitized 316 stainless steel, and to determine the influence of sensitization on the suitability of 316 stainless steel for orthopedic application.